Retreat patterns and dynamics of the Sentralbankrenna glacial system, Central Barents Sea

Mariana Esteves[1*], Lilja R. Bjarnadóttir[2], Monica C. M. Winsborrow[1], Calvin S. Shackleton[1], Karin Andreassen[1]

[1] CAGE - Centre for Arctic Gas Hydrate, Environment and Climate, Department of Geosciences, UiT the Arctic University of Norway, 9037 Tromsø, Norway.

[2] Geological Survey of Norway (NGU), Postboks 6315 Sluppen, 7491, Trondheim, Norway.

[*] mariana.esteves@uit.no

Abstract

The Barents Sea Ice Sheet (BSIS) is a good palaeo-analogue for the present day West Antarctic Ice Sheet. Both were marine-based ice sheets, particularly vulnerable to ocean warming and sea-level rise. Understanding the BSIS ice dynamics and patterns of retreat since the Last Glacial Maximum (LGM) is useful in developing our knowledge of spatial and temporal variations during marine-based ice sheet retreat. While the western margins of the Barents Sea have been extensively studied, few studies have focused on the central regions, which hosted key ice stream tributaries and major ice domes and divides. Presenting a new high-resolution (5 m) bathymetric dataset, this glacial geomorphological study focuses on the Sentralbankrenna palaeo-glacial system in the central Barents Sea. A large number of grounding zone wedges, mega-scale glacial lineations and areas with tunnel valleys and palaeo-subglacial basins were identified. These form the basis for a six-stage reconstruction of ice stream retreat through deglaciation since the LGM. In reconstructing the retreat of the Sentralbankrenna Ice Stream, we document the rapid but highly spatially variable pattern of retreat of a marine-based ice sheet margin. The presence of several tunnel valleys and interconnected palaeo-subglacial basin systems indicates an abundance of meltwater, likely to have been stored and released through several discharge events, significantly influencing the ice stream margin dynamics. This study provides insight into the behaviour and dynamics of ice during the late stages of the BSIS deglaciation within the central Barents Sea, increasing our understanding of grounding line processes.

Keywords:

Late Quaternary; Deglaciation; Barents Sea Ice Sheet; Glacial geomorphology; Sentralbankrenna palaeo-Ice Stream; GZW; MSGL; Marine-based ice sheet; Ice stream reconstruction; Glacial dynamics.

1. Introduction

Ice streams are important and highly dynamic components of contemporary- and palaeo-ice sheets, transporting large amounts of ice and sediment from the ice sheet interior to the margins (Bamber et al., 2000); thereby significantly influencing the stability of the ice sheet (Bennett et al., 2003). Insight into the processes that occur at ice margins is of vital importance for understanding ice-ocean interactions and the consequences of ocean warming (Alley et al., 2005; Bindschadler, 2006; Pritchard et al., 2009). In particular, processes occurring at the grounding zones (where grounded ice loses contact with the bed), where a large amount of mass is lost by calving and melting (Jenkins and Doake, 1991; Rignot and Jacobs, 2002). This, in conjunction with other climatic changes, can lead to acceleration of ice streams, promoting destabilisation in the interior of the ice sheet (Oppenheimer, 1998; Rignot et al., 2004; Shepherd et al., 2004; Bindschadler, 2006). Present day Antarctic and Greenland Ice Sheets are vulnerable to oceanographic and climatic changes, such as increasing surface water temperatures and atmospheric warming, particularly at their ocean margins, thus it is essential to develop our understanding of the processes and mechanisms that influence the spatial and temporal retreat of ice streams.

During the Last Glacial Maximum (LGM; 18-21 cal ka BP) a large marine-based ice sheet covered the Barents Sea, extending to the western continental shelf break (fig. 1; Svendsen et al., 2004). The Barents Sea Ice Sheet (BSIS) is considered a good palaeo-analogue for marine-based ice sheets (Siegert et al., 2002) such as the present-day West Antarctic Ice Sheet (WAIS). They have many similarities, both are marine-based with their beds mostly below sea-level, both are overlying sedimentary bedrock, and had similar sizes and extents during the LGM (Andreassen and Winsborrow, 2009). However, unlike the WAIS, the BSIS completely deglaciated following the LGM.

Details of its deglaciation history are preserved in the glacial sediments and landforms imprinted onto the seafloor of the Barents Sea and have been extensively studied in southwest Barents Sea and parts of the Svalbard margin (fig. 1; i.e. Vorren and Kristoffersen, 1986;

Elverhøi et al., 1993; Solheim et al., 1996; Landvik et al., 1998; Dowdeswell et al., 2010; Winsborrow et al., 2010; Rüther et al., 2012; Ingólfsson and Landvik, 2013; Andreassen et al., 2014; Bjarnadóttir et al., 2014; Piasecka et al., 2016). In contrast, the central Barents Sea remains poorly studied, despite it being the site of a major ice dome and ice divides for the BSIS, as well as hosting several ice streams and their tributaries.

Ice streams leave a series of characteristic geomorphic imprints on the seafloor, which document the spatial and temporal patterns of retreat. By studying these we can gain valuable insights into the processes and mechanisms controlling ice stream behaviour (Stokes and Clark, 2001; Livingstone et al., 2012a).

Until recently, there has been a particular scarcity of bathymetric data available from the central Barents Sea due to a political Norwegian-Russian border dispute. This is in contrast to that available from the southwestern Barents Sea where several surveys have been undertaken. We present a high-resolution dataset from the central Barents Sea, immediately west of the border between Norway and Russia (fig. 1). Focusing on the Sentralbankrenna Ice Stream and its glacial system, which encompasses the adjacent bank areas Sentralbanken and Thor Iversenbanken. The Sentralbankrenna Ice Stream was a tributary to Bjørnøyrenna during the LGM and an important area during the final stages of the central BSIS deglaciation. In this paper, we present glacial geomorphological mapping from the bed of the Sentralbankrenna palaeo-Ice Stream, which is then interpreted to determine ice flow patterns and ice dynamics during deglaciation. We document rapid, episodic ice stream retreat associated with periods of increased ice margin break up punctuated by margin stillstands or short readvances. Subglacial meltwater was abundant in this area and is suggested to have significantly influenced the overlying ice by facilitating fast flow both for the Sentralbankrenna and Bjørnøyrenna Ice Stream.

2. Glacial and regional setting/Study area

The Barents Sea is the largest epi-continental sea in the world and is characterised by relatively shallow banks (100-200 mbsl) and large, deep troughs (300-500 mbsl; fig. 1). Investigations into the large trough mouth fans at the shelf break suggest that the Barents Sea has undergone multiple glaciations during the Cenozoic (Vorren et al., 1988; Vorren and Laberg, 1997), with the most recent having taken place in the Late Weichselian (Landvik et al., 1998; Svendsen et

al., 2004). During this final glaciation, the BSIS reached the continental shelf break (fig. 1; Svendsen et al., 1999), depositing sediments along the northern and western continental slopes forming large trough mouth fans composed of glacigenic debris flow deposits (Laberg and Vorren, 1995; Dowdeswell et al., 1996; Kleiber et al., 2000; Andreassen et al., 2004).

The BSIS was a multi-domed ice sheet, and the ice divides for the LGM and early phase of deglaciation have been extensively studied and derived based on empirical data-sets (e.g. Bondevik et al., 1995; Forman, 2004; Ottesen et al., 2005) and glacial-isostatic adjustment modelling (e.g. Lambeck, 1995; 1996; Auriac et al., 2016). These studies indicate that one of the ice domes was located over Storbanken, in the northern Barents Sea, and may have extended over Sentralbanken (fig. 1; Bjarnadóttir et al., 2014; Patton et al., 2015; Piasecka et al., 2016). During the late phase of glaciation, the ice divide over Storbanken migrated northwest, into separate ice domes over e.g. Hinlopenstretet (Dowdeswell et al., 2010) and Nordaustlandet (Hormes et al., 2013).

During the LGM several ice streams occupied the cross shelf troughs; although not necessarily active synchronously these transported ice and sediments from the inner sectors of the BSIS to its margins (Ottesen et al., 2002; Andreassen et al., 2008; Bjarnadóttir et al., 2014; Patton et al., 2015; Vorren and Laberg, 1997). Empirical and modelling evidence suggest that during maximum glacial extent these ice streams were not topographically constrained, with the Bjørnøyrenna Ice Stream flowing straight from eastern Barents Sea where there was an ice divide located over the south east Barents Sea (Bjarnadóttir et al., 2014; Piasecka et al., 2016; Patton et al., 2016). However, throughout deglaciation the BSIS underwent several changes in flow regime, ice dynamics, and reorganisation of ice dome/divide and ice stream locations, as well as, ice stream flow switching (Polyak et al., 1995; Andreassen et al., 2008; Winsborrow et al., 2010, 2012; Bjarnadóttir et al., 2014; Patton et al., 2015). Towards the end of the deglaciation, as the ice sheet thinned, flow became more topographically controlled (Andreassen et al., 2008; Winsborrow et al., 2010, 2012; Bjarnadóttir et al., 2014; Patton et al., 2015).

The largest Barents Sea palaeo-ice stream was the Bjørnøyrenna Ice Stream, a major outlet of the BSIS with a catchment area in excess of 350,000 km^2, which occupied Bjørnøyrenna (fig. 1; Winsborrow et al., 2010; Andreassen et al., 2014; Bjarnadóttir et al., 2014). It is likely that this ice stream had several tributaries, including the fast flowing ice coming from Sentralbankrenna, within our study area (fig. 1; Bjarnadóttir et al., 2014). Given the area of

Sentralbankrenna (>30,000 km^2), the behaviour and flow patterns of this tributary likely played a significant role in controlling ice dynamics and the flow regime of the Bjørnøyrenna Ice Stream.

The glacial imprints left by the Bjørnøyrenna Ice Stream have been extensively studied (e.g. Vorren and Laberg, 1997; Andreassen et al., 2008; Andreassen and Winsborrow, 2009; Rüther et al., 2011; Andreassen et al., 2014; Bjarnadóttir et al., 2014; Piasecka et al., 2016), and suggest dynamic ice margins and rapid, but episodic retreat patterns throughout the trough during deglaciation since the LGM. Bjarnadóttir et al. (2014) and Newton and Huuse (2017) suggest a number of former ice margin positions throughout the central Barents Sea (fig. 1) based on ice marginal features such as grounding zone wedges and retreat ridges. Several meltwater features are also described in the central Barents Sea, including in Sentralbankrenna and Thor Iversenbanken (Bjarnadóttir et al., 2017; Newton and Huuse, 2017).

Deglaciation in the western part of the Barents Sea initiated by 17.5 cal ka BP (Rüther et al., 2011). Due to lack of data in the central Barents Sea, there are large uncertainties about the timing of full deglacial conditions over this region. Hughes et al. (2015) provide estimates (min, med, max) of ice margin extents, suggesting that the central Barents Sea became ice free sometime between 16-12 cal ka BP. We suggest that our study area would have been undergoing deglaciation after 16 cal ka BP, based on ice margin extents of Hughes et al. (2015) and Winsborrow et al. (2010; fig. 1).

3. Datasets and method

The bathymetric data presented herein was provided by the MAREANO Programme (www.mareano.no). The original dataset has a horizontal resolution of 5 m, with the multibeam covering an area of approximately ~17,000 km^2 over Sentralbankrenna and the northwestern flanks of Thor Iversenbanken (fig. 1). The horizontal grid size was decreased during the mapping stage to a resolution of 25 m to focus on the larger-scale glacial features. The bathymetric dataset was used to carry out detailed mapping of the distribution and morphology of glacial sediments and landforms on the seafloor (fig. 2 A). The landforms were mapped and visualised using Esri ArcMap v10.1 and QPS Fledermaus. The International Bathymetric Chart of the Arctic Ocean (IBCAO; version 3.0), with a grid size of 500 m, consisting of several

bathymetric datasets of varying resolution (Jakobsson et al., 2012), was used to give a broader overview of the seafloor bathymetry.

4. Results and interpretation

The key glacial landforms identified in the study area are described and interpreted below (fig. 2 A). The results are then synthesised (fig. 2 B and E), providing new insights into the spatial and temporal variations of the ice margin and the distribution of fast and slow flowing ice within the Sentralbankrenna glacial system during the final stages of BSIS deglaciation, as well as the influence of this glacial system on the wider BSIS.

4.1. Sedimentary deposits: Large grounding zone features

4.1.1. Description

The most prominent, large-scale features identified in Sentralbankrenna are nine, trough-transverse sediment ridges or wedges (fig. 2 A-G; table 1). The southernmost (farthest downstream) sedimentary deposit 1 (labelled GZW 1 in fig. 2 B) is a large and prominent wedge-shaped feature at a minimum 295 m water depth and extending across the mouth of Sentralbankrenna (fig. 2 B and C). It is visible on both the high resolution multibeam and the IBCAO data (fig. 2 A) and has a height of ~35 m relative to the seafloor downstream of the feature. Sedimentary deposit 1 has a dome-like shape and a slightly steeper ice-distal, downstream slope compared its ice-proximal, upstream slope (fig. 2 B and C; table 1). This sedimentary deposit extends across 100 km of the trough in a NE-SW direction. It has a width of ~35 km, at the widest point visible in the multibeam dataset; however, measurements taken using IBCAO suggest that it extends beyond this high resolution dataset, having a width of ~60 km. Bjarnadóttir et al. (2014) discuss multibeam and subsurface data from this area and conclude that this deposit is a composite landform, consisting of at least four generations of grounding zone wedges, which have an acoustically transparent internal structure. Overprinting the ice proximal side of sedimentary deposit 1, are several large elongated linear features (previously described and interpreted in Bjarnadóttir et al., 2014; cf. section 4.2.; fig. 2 A and B). At its northern extent there is a deep erosional channel that cuts through the sedimentary wedge (cf. section 4.3., fig. 2 A and B).

Sedimentary deposit 2 (fig. 2 B; GZW 2) joins the first sedimentary deposit on its west but is orientated in a more NW-SE direction and is not as large as sedimentary deposit 1. Deposit 2 is less prominent in the bathymetric dataset, mainly due to a heavily scoured surface. With its crest at a slightly deeper water depth (~305 m) than GZW 1, it extends for ~45 km. It has a slightly asymmetric wedge-like shape, with an ice distal slope of ~0.20° that is ~10 m high from the level of the seafloor, downstream of the wedge. At its widest part, sedimentary deposit 2 is at least ~15 km (fig. 2 D). It lies directly upstream from the deep elongated linear features overprinting the eastern side of grounding zone deposit 1 (previously described and interpreted in Bjarnadóttir et al., 2014; cf. section 4.2.; fig. 2 A; GZW 1). In its western part several deep channel-like features appear to have cut through the upstream part of the deposit (cf. section 4.3), giving this part of the deposit a steeper ice proximal slope, in contrast to the rest of sedimentary deposit 2 (table 1).

Sedimentary deposit 3 (fig. 2 B and E; GZW 3) is located in mid-Sentralbankrenna at a minimum water depth of ~265 m and, similar to sedimentary deposit 2, has a slightly asymmetrical wedge-like profile, with a steeper downstream, ice distal slope (table 1). The surface of the deposit is heavily grooved, having both been overprinted by and overprinting many curvilinear furrows. The extent of the full deposit is unclear due to this heavy scouring, however, it seems that it extends for at least ~80 km, with a NW-SE orientation in its western, more prominent part, and more NE-SW orientation in its eastern part, which extends towards sedimentary deposit 4. It is ~26 m high and up to ~15 km wide.

Adjacent to the eastern-most part of sedimentary deposit 3, is the much smaller yet pronounced sedimentary deposit 4, which is located at a water depth of ~235 m (fig. 2 E; GZW 4). It is ~14 km long with a height of ~30 m in relation to the seafloor downstream (fig. 2 G; table 1). This deposit has a W-E orientation and a large quantity of furrows overprint and possibly have reworked its western side and thus, maybe concealing its full extent (fig. 2 E). Moreover, it has been heavily overprinted by large elongated parallel linear features on the ice proximal side (fig. 2 E; cf. section 4.2).

Sedimentary deposit 5 is located on the eastern part of Sentralbankrenna and has a distinct asymmetrical wedge-like shape (figs. 2 E, G and 3 A; GZW 5). Based on its morphology and seafloor expression the wedge can be divided into eastern and western sections (fig. 3 A). It extends in a NW-SE direction for ~35 km, and is located in water depths of ~215 m at its eastern side and ~250 m at its western side. The eastern side of the deposit has a clear asymmetric

shape, with a width of ~30 km at its widest point, a height of ~31 m and a steeper ice distal slope (figs. 2 G, 3 A and B; table 1). The eastern side of this deposit extends slightly north in the middle of the feature (between the western and eastern side), forming a wedge-shaped ridge dividing it from its western counterpart (fig. 2 A).

The western side of sedimentary deposit 5 is less pronounced than its eastern side and has a radial, fan-like geometry, with a height of ~10 m, width of ~20 km and a less steep overall profile (fig. 3 A and C; table 1). A clear break in slope can be traced along the whole of the ice distal side of this western section of the wedge (indicated by the red arrow in fig. 3 A and C), perhaps indicating a second wedge-like feature. The extent of the lower wedge is unclear, although it has a similar overall profile to that which overlies it, with a steep ice distal slope and a height and width of ~10 m and ~8 km, respectively (figs. 2 E, 3 A and C; table 1). This western side of sedimentary deposit 5 is located in a deeper part of trough, and the fan-shaped deposits are heavily overprinted by, and themselves overprint, many semi-parallel curvilinear furrows (cf. section 4.6). In the middle section of sedimentary deposit 5, between the western and eastern sides of the deposit, are several smaller fan-shaped deposits. These are greater in height but smaller than the fan-shaped western margin of deposit 5 (heights ~20 m, widths ~1.5 km; fig. 3 A).

North of deposit 5 is a large and prominent sedimentary deposit 6 (figs. 2 E and 3 D; GZW 6). It is located at a much shallower depth than sedimentary deposits 1-5, with the crest of the sedimentary deposit at ~190 m water depth. This deposit appears to be well preserved with little indications of overprinting from other features, except for a small number of elongated linear features imprinted into its ice proximal slope (cf. section 4.3) and some randomly orientated furrows on the crest (cf. section 4.6). The wedge extends in an ESE-WNW direction for ~37 km, is ~15 km at its widest point and has a clear asymmetrical shape (fig. 2 G; table 1) with many lobate features making up its margin (fig. 3 D and E). The extent of the western-most part of the wedge is a little unclear as it fades into an area dominated by smaller sedimentary ridges (cf. section 4.4).

Sedimentary deposit 7 (fig. 2 E; GZD 7) is to the west of the sedimentary deposit 6, located in the northwestern part of Sentralbankrenna at a water depth of ~160 m. Unlike the sedimentary deposits previously described, it is more symmetrical, considerably higher and narrower (table 1), and height of ~50 m in relation to the seafloor downstream. It extends for ~20 km in a W-E

direction and is ~4 km at its widest section. In the areas up and downstream of this large sedimentary deposit there are many small, pronounced sedimentary ridges (cf. section 4.4).

Sedimentary deposit 8 (GZD 8; fig. 2 B), on the north-western flanks of Thor Iversenbanken at a water depth of ~240 m, has similar morphological characteristics to sedimentary deposit 7 (table 1). This deposit is composed of three closely spaced, symmetrical sedimentary deposits, orientated in a NE-SW direction, which have widths and heights ranging from 200-340 m and 3-11m, respectively. These have been previously described and interpreted by Bjarnadóttir et al., (2014).

On the northern flanks of Thor Iversenbanken, connecting with the mid-section of Sentralbankrenna, is sedimentary deposit 9 (GZD 9; fig. 2 B and E), which is ~45 km long and its surface has been heavily scoured by both curvilinear and randomly orientated furrows (fig. 2 B and E). At its widest point (in the northern most part of Thor Iversenbanken), it has a width of ~8 km and height of ~25 m (table 1), however as it extends into the north-western part of Thor Iversenbanken, its shape and seafloor expression becomes less pronounced.

4.1.2. Interpretation

We identified nine large sedimentary deposits (fig. 2 A-G; table 1) and interpret these to indicate former grounding line positions. Based on their morphology and seafloor expression, two main types of deposits are identified within the Sentralbankrenna glacial system. The first have clear wedge-like forms and are interpreted to be grounding zone wedges (GZWs). In contrast, the second type of deposits are smaller, narrower and lacking a pronounced wedge-like form and so, while they are interpreted to also represent ice marginal deposits these will be referred to as grounding zone deposits (GZDs). Of the mapped landforms sedimentary deposits 1-6 are interpreted to be GZWs and will henceforth be referred to as GZW 1-6 (fig. 2 B and E, table 1). This interpretation is consistent with that of Bjarnadóttir et al. (2014) who previously interpreted GZW 1-3 in our study. Sedimentary deposits 7-9 are interpreted to be GZD and will henceforth be referred to as GZD 7-9 (fig. 2 B and E, table 1). We propose that the steep, narrow GZDs 7, 8 and 9 (fig. 2 E) are large recessional moraines (GZD 8 previously described and interpreted in Bjarnadóttir et al., 2014). Such landforms typically form at tidewater ice cliffs through a combination of processes, such as squeeze-push from under the ice mass and the deformation of the sediment beneath (Powell, 1981; 1991; Powell and Domack, 1995; Powell

and Alley, 1997) and are typical for inter-ice stream areas (Kirkbride and Warren, 1997; Ottesen and Dowdeswell, 2009). There is a noticeable lack of scouring both downstream and upstream of these features, and it is therefore likely that the ice here was slower moving, with little calving occurring at the margin.

GZWs have been observed and extensively studied in many locations on high-latitude palaeo-ice stream beds (e.g. Mosola and Anderson, 2006; Ó Cofaigh et al., 2008; Bjarnadóttir et al., 2013; 2014; Rydningen et al., 2013). These are ice-marginal landforms, formed at the grounding zone of fast-flowing ice streams (Powell and Domack, 1995; Dowdeswell et al., 2008) and are suggested to temporarily stabilise the ice stream grounding line to the effects of sea-level rise (Alley et al., 2007; Anandakrishnan et al., 2007).

GZW 1-6 all have similar morphological and acoustic characteristics: slight-to-prominent asymmetric profiles (steeper ice-distal slopes), a relatively high length-to-height ratio and are acoustically transparent, which are typical of GZWs (Powell and Domack, 2002; Dowdeswell and Fugelli, 2012; Batchelor and Dowdeswell, 2015). These wedge-like deposits are formed through rapid deposition and deformation of subglacial sediment at the ice margin, and its subsequent redistribution through gravity flow processes (Powell and Alley, 1997; Dowdeswell and Fugelli, 2012). Their acoustic transparency reflects the unsorted nature of the diamictic debris being deposited at the grounding zone (Batchelor and Dowdeswell, 2015). The presence of GZWs in the palaeo-record enables identification of ice margin positions during stillstands or re-advances (from decades to centuries), and their morphology and relation to other geomorphological features can provide clues to the overlying ice dynamics and retreat patterns (e.g. Mosola and Anderson, 2006; Alley et al., 2007; Anandakrishnan et al., 2007; Dowdeswell et al., 2008; Ó Cofaigh et al., 2008; Dowdeswell and Fugelli, 2012; Livingstone et al., 2012a; Livingstone et al., 2016a). Thus, the six GZWs in Sentralbankrenna (GZW 1- 6) indicate that ice streaming within this trough experienced periods of ice break up and rapid retreat, punctuated by stabilisation during stillstands or readvances.

GZW 1 is the largest within this dataset and is composed of four generations of deposition (Bjarnadóttir et al., 2014). From its position in relation to the rest of the features, we suggest this to be the oldest ice marginal landform within the dataset, deposited by ice flowing in a north-west to south-east direction. GZW 2 is not as prominent as the other GZW1-4, perhaps indicating that the ice margin was stable in this position for a relatively short period, when the ice stream was undergoing fast retreat and the grounding line only just grounded. Alternatively,

312 it may represent changes in the flux of sediment to the grounding line. The northern sections of
313 GZW 1 and 2 have been breached by several channels (c.f. section 4.3), indicating that
314 meltwater was likely to have been present during the formation of these GZW.

315 GZW 3 is heavily scoured and overprinted by curvilinear furrows (fig. 2 B and E, c.f. section
316 4.6.). To the east, GZW 4 is overprinted by elongated linear features on its ice-proximal side
317 (fig. 2 E, c.f. section 4.2.), suggesting that this was formed under fast flowing ice (Ó Cofaigh
318 et al., 2005; Graham et al., 2010), and that the ice was still streaming during or after the final
319 stages of its formation.

320 The eastern side of GZW 5 (fig. 5A) represents a classic GZW, with an asymmetrical profile
321 and high length-to-height ratio. We suggest that the grounding line of the Sentralbankrenna Ice
322 Stream was stable in this area for some time allowing a large and clear GZW to develop. In
323 contrast, the western part of GZW 5 resembles a large radially shaped fan, with a clear slope
324 break at its downstream margin. The western side of GZW 5 may represent a large grounding
325 line fan (fig. 3 A), indicating that this part of the deposit was highly influenced by meltwater,
326 with sediment deposition either due to subglacial meltwater derived sediment plumes,
327 subaqueous debris flows, or a combination of the two. This is likely to be a composite feature,
328 formed and reshaped during two stillstand/readvance events, with the sediment fans having
329 been deposited by a relatively ice proximal meltwater plume from a subglacial meltwater
330 conduit ending at the ice margin. In between the western and eastern side of GZW 5 there are
331 many smaller grounding line fans along its ice distal slope (fig. 5 A). Similar features have been
332 described as part of GZWs in Kveithola, western Barents Sea (Bjarnadóttir et al., 2013) and in
333 Storfjordrenna, NW Barents Sea (Shackleton et al., Submitted), and interpreted as intermediate
334 GZWs, heavily influenced by meltwater activity at the former ice margin. We propose that
335 GZW 5 also represents such an intermediate GZW. Whilst the eastern and western part of this
336 sedimentary wedge have been described as part of the same deposit, it is clear that the ice
337 margin experienced different ice dynamics along its front. It is possible that a large embayment
338 in the ice margin formed over the western part of GZW 5 due to its position within the deeper
339 section of the trough, enabling the formation of the GZW radial fan-shaped geometry.

340 Further north, GZW 6 is a large and very prominent feature on the seafloor, with a very clear
341 terminus on its ice distal side (fig. 3 D). Based on its location, we suggest that this GZW was
342 formed during the late stages of deglaciation in this trough. This is consistent with interpretation
343 from Newton and Huuse (2017).

344

345 4.2. Linear elongated features: Mega-Scale Glacial Lineations

346 *4.2.1. Description*

347 Within Sentralbankrenna we identify five areas with differing orientations where assemblages
348 of broadly parallel linear elongated ridge-groove features can be seen on the seafloor (fig. 2 A,
349 B and E; MSGL 1-5). The first area (MSGL 1; figs. 2 B and 4 A) is located on the ice proximal
350 side of GZW 1 and is characterised by the largest amplitude ridge-groove features mapped in
351 Sentralbankrenna. Here the features have a predominant NE-SW orientation, with ridges ~880-
352 2680 m wide, ~25-42 km long, heights between ~2-3 m, and with elongation ratios
353 (width:length) ranging from 1:15 to 1:28 (fig. 4 B). The second area (MSGL 2) of pronounced
354 parallel elongate ridge-groove features is located between GZW 1 and GZW 2, slightly north
355 of area 1 (figs. 2 B and 4 A), and has been previously described and interpreted by Bjarnadóttir
356 et al., 2014. These pronounced parallel elongate ridge-groove features extend in an ENE-WSW
357 direction with an individual length of ~11-14 km, ~350-1200 m wide, 2-8 m high, and
358 elongation ratios ranging from 1:12 to 1:32 (fig. 4 C). Both the first and second area of elongated
359 features are located in the deepest part of the study area (area 1 water depth is ~295 m; area 2
360 water depth is ~320 m).

361 The third area (MSGL 3; figs. 2 E and 4 D) is located in the eastern part of mid-
362 Sentralbankrenna, where very clear parallel linear ridge-groove features can be observed
363 overlying and terminating on top of GZW 5 (fig. 4 D). These landforms are orientated in a
364 NNE-SSW direction and are smaller than those in areas 1 and 2, ~5-10 km long, ~180-530 m
365 wide, heights ~2-7 m (fig. 4 E), with elongation ratios between 1:12 and 1:53. The fourth area
366 (MSGL 4; fig. 2 E) is located on the ice proximal slope of GZW 6, in the north-easternmost
367 part of Sentralbankrenna. Here, large ridge-groove linear features are imprinted onto the
368 seafloor, with lengths of ~4-8 km, widths of ~240-640 m, heights of ~1-6 m, and elongation
369 ratios between 1:12 and 1:32. These features are oriented in a NE-SW direction. The fifth area
370 (MSGL 5; fig. 2 E), is west of the fourth, just south of sedimentary deposit 7, in the northwestern
371 part of Sentralbankrenna. In this area, the ridge-groove features are oriented in an ENE-WSW
372 direction, extend ~2.7-3.1 km in length, are ~85-100 m wide, have heights between ~0.4-0.8 m,
373 and elongation ratios ranging from 1:28 to 1:33. The linear features in the fifth area are
374 relatively short and cover only a small area, unlike similar features found in other areas. This
375 area is also surrounded by many small sedimentary ridges (cf. section 4.4).

376

377 *4.2.2. Interpretation*

378 The linear elongated ridge-groove features in areas 1-5 are interpreted to be mega-scale glacial
379 lineations (MSGLs; henceforth areas 1-5 are now referred to as MSGL 1-5). MSGLs are formed
380 beneath fast flowing ice (Clark 1993), and have been widely used to identify the location of
381 palaeo-ice streams in formerly glaciated areas (e.g. Stokes and Clark, 1999; 2001; Graham et
382 al., 2009).

383 The MSGLs within Sentralbankrenna show different scales and different positions in relation
384 to other glacial geomorphological features. MSGLs 1 to 4 are all located on the ice-proximal
385 slope of GZWs, thus indicating that the ice overlying these areas was fast flowing during or
386 after the deposition of the wedges (Ó Cofaigh et al., 2005; Dowdeswell et al., 2008; Graham et
387 al., 2010). MSGL 5, located downstream of GZD 7, is considerably smaller than the other
388 MSGLs, and has a differing orientation in comparison to the ridge features around it (cf. section
389 4.4). It is possible that MSGL 5 are older features that have been partially buried by younger
390 sedimentary ridge features.

391 MSGLs 1 are considerably larger than the other MSGLs, both in terms of the area that they
392 cover and also the amplitude of the features, and are likely related to a period when the
393 Sentralbankrenna Ice Stream was fast flowing and depositing GZW 1. MSGLs 2 immediately
394 upstream, have a slightly different orientation, suggesting a switching in ice stream flow
395 direction within the trough during ice stream retreat from GZW 1 to GZW 2. Subglacial
396 meltwater, in conjunction with easily deformable sediment (Fowler et al., 2010), may have
397 played a significant role in enabling the formation of the MSGLs in area 1 and 2. In support of
398 this, several meltwater channels have been previously identified in the areas adjacent to the
399 MSGLs (Bjarnadóttir et al., 2012; 2014; 2017; this study, c.f. section 4.3.), indicating that there
400 was abundant meltwater discharging into this area.

401 The formation of MSGLs 3 and 4 was likely to have occurred simultaneously to the formation
402 of GZW's 4 and 6, respectively. Meanwhile, the timing of the formation of MSGL 5 and its
403 relationship with the surrounding landforms remains more uncertain. No further MSGLs within
404 Sentralbankrenna, or on the ice proximal sides of GZW 2 and 3, were observed during this
405 study. Rather than reflecting a lack of fast flowing ice in this area, we suggest that MSGLs may

have been present but have been subsequently obscured by heavy scouring of the seafloor (fig. 2 A, B and E).

4.3. Seafloor channels and basins: Meltwater features

4.3.1. Description

Located between GZW 1 and GZW 3 are three areas with channel-like furrows and depressions on the seafloor (fig. 2 A and B). The first area is located in the northern part of GZW 2, upstream of GZW 1 (fig. 5 A). Here, several channels were identified, extending on the seafloor for ~7-20 km in length, with an undulating long profile (fig. 5 B). The channels have varying widths and depths, 80-155 m and 3-10 m, respectively (fig. 5 B and C). All the mapped channels in this area are orientated NE-SW and are inter-linked in a large anastomosing system (fig. 5 A), cutting through the northern part of GZW 2 and GZW 1 (fig. 2 B). These have been described and interpreted by Bjarnadóttir et al. (2012; 2017).

In the western part of Thor Iversenbanken, adjacent and to the east of MSGLs 1, is a long single channel (fig. 5 D), oriented SE-NW. This channel extends ~4 km on the seafloor, is ~60 m wide and 3 m deep (fig. 5 E). There is also an elongated, relatively straight, ridge running parallel to this channel (fig. 5 D and E), with the same length but with a width and height of ~92 m and ~2 m, respectively. To the west of this area is a large depression on the seafloor (fig. 2 A), ~3.5 km long, ~1.8 km wide, with a depth of ~40 m.

East of MSGLs 2, in the north-western flanks of Thor Iversenbanken, is a third channel and basin area (figs. 2 B and 5 F). Here, several channels merge in a dendritic manner downstream of three depressions, and cut through a number of small sedimentary ridges (c.f. section 4.4), previously identified by Bjarnadóttir et al. (2012; 2014; 2017). These channels are orientated SE-NW towards the trough, where they end abruptly, close to the slope break. The main channel in this area is ~310 m wide, ~32 m deep and ~50 km long (fig. 5 G and H). The northern-most channel in the basin area splits into two, with one channel connecting to the depressions from the northeast, subsequently feeding into the main channel and the other, a single meandering channel, extending ~40 km, ~150 m wide, and ~7 m deep (fig. 5 I) towards the trough. The depressions on the seafloor are situated upstream of the main channel and are relatively shallow, < 20 m deep, with basin-like shapes and lengths/widths ranging from, 2.3-4 km and 1-1.5 km, respectively.

437

438 *4.3.2. Interpretation*

439 The meltwater channel network north of GZW 2 (fig. 5 A) is interpreted to be an extensive
440 system of tunnel valleys, which have been previously described by Bjarnadóttir et al. (2012;
441 2017). These features are erosionally formed by subglacial meltwater at the base of the ice sheet
442 (Ó Cofaigh, 1996; Kehew et al 2012; Greenwood et al 2016). The channels have breached
443 GZWs 1 and 2 (fig. 2 B), indicating that they may have been formed gradually over time and
444 have been active during the build-up of both GZWs 1 and 2.

445 The smaller channel on the western flanks of Thor Iversenbanken (fig. 5 D) is interpreted to
446 have formed subglacially under a channelised meltwater regime and the elongated ridge running
447 parallel to it is interpreted as an esker. It is possible that this esker may have formed during a
448 period when the ice was slower moving in this area or possibly even close to the ice margin,
449 during which the meltwater conduits remained stable for sufficient time for esker to form.
450 Similar formation processes have been suggested for the formation of eskers observed in
451 Canada (Storrar et al., 2014). We suggest that the large depression west of this channel and
452 esker (fig. 2 A) may have served as a subglacial basin once hosting a subglacial lake, however,
453 further subsurface and empirical data is required to verify this.

454 East of MSGL 2 a series of arborescent channels form a dendritic hydraulic network
455 downstream of three basins. These channels have been previously described and interpreted by
456 Bjarnadóttir et al., (2012; 2017) and Newton and Huuse (2017) to be tunnel valleys formed
457 gradually over time and to have been active close to the ice margin. The main channel has an
458 undulating long profile (fig. 5 G), with a shallowing at the mouth of the channel, indicating that
459 there must have been significant pressure from overlying ice to cause subglacial water to be
460 driven uphill. The channel ends abruptly when it enters the trough, either indicating the channel
461 ending at the margin, or suggesting a possible boundary, or shear margin, between the slower
462 inter-ice stream ice on Thor Iversenbanken and the streaming ice of the Sentralbankrenna Ice
463 Stream (c.f. section 5.1.2.).

464 The basins upstream of the dendritic channel network are inferred to have hosted palaeo-
465 subglacial lakes, based on their geomorphic properties (e.g. as described in Livingstone et al.,
466 2012b) and the presence of channels leading into and out of the basins, as well as evidence of
467 channels cutting through some of the basins. We suggest that these lakes would have discharged

a large amount of meltwater into the channels and may have undergone several periods of drainage and infilling, similar to those identified in Antarctica (Fricker and Scambos, 2009) and Greenland (Palmer et al., 2013). Similar palaeo-subglacial lakes have been described elsewhere, for example in Canada, by Christoffersen et al. (2008) and Livingstone et al. (2016b). While these channels and basins are not located at the onset zone of the ice stream, we propose that the presence of these channel areas at the sides of the trough may have played a significant role for the development of MSGLs and/or in the facilitation of ice streaming in the trough (e.g. King et al., 2009; Fowler et al., 2010), providing a mechanism for rapid discharge of meltwater into the trough. Running perpendicular to the channels in this area are several sedimentary ridges (cf. section 4.4; Bjarnadóttir et al., 2014), which have been breached at several points, suggesting that the channels in this area were active during a period of ice retreat in this area. Furthermore, Bjarnadóttir et al. (2012; 2017) suggested that the tunnel valleys in this basin and channel area (fig. 5 F) may have undergone several outburst floods, which we suggest may have been promoted by the presence of the palaeo-subglacial basins further upstream.

Meltwater plays an important role in ice sheet and ice stream dynamics, facilitating fast ice flow for overlying ice (Hulbe and Fahnestock, 2004; Bell, 2008; Greenwood et al., 2016). The channels observed in Sentralbankrenna and on Thor Iversenbanken must have formed subglacially since the ice stream had a marine margin.

4.4. Sedimentary ridges: Retreat ridges

4.4.1. Description

Within the bathymetric dataset there are four distinct areas with small sedimentary ridges; linear, parallel features, with a symmetrical shape. The first area is located in the channel and basin area, east of GZW 2, where four large ridges are clearly visible running perpendicular to the channels (fig. 5 F; Bjarnadóttir et al., 2014), with widths ranging from 400-600 m and heights between 8-17 m, they have a regular spacing between 1-3 km (Bjarnadóttir et al., 2014; 2017). Between these larger ridges, there are many slightly smaller ridges, with widths and heights ranging from 110-240 m and 3-14 m, respectively, as well as a regular spacing of 150-350 m (fig. 5 J). The sedimentary ridges in this area occur 1-3 km upstream from a visible slope break between Thor Iversenbanken and Sentralbankrenna, and at a water depth ranging between 260-300 m.

The second area with several small sedimentary ridges is located in the northern-most flanks of Thor Iversenbanken, to the east of grounding zone deposit 9 (fig. 2 A and E) in water depths ranging from 220-235m. Short and narrow ridges were also identified with a more north-south orientation, with widths and heights ranging from 84-405 m and 4-12 m, respectively.

To the west of GZW 5, downstream of GZD 7, is sedimentary ridge area three, where there are several ridges with an approximately W-E orientation, widths ranging from 95-155 m and heights of 3.5-6 m, in water depths ranging from 245-270 m (fig. 6 A and B). North of this area, both up- and down-stream of the GZD 7 is sedimentary ridges area four, which, in comparison to the other areas, is located at a much shallower water depth between 180-230 m (fig. 2 E). Here, many sedimentary ridges are observed with an approximate NE-SW direction, widths of 100-185 m and heights of 3.5-8 m.

4.4.2. Interpretation

The small, linear, semi-parallel sedimentary ridges identified in the study area have a semi-regular spacing, and are interpreted to be retreat ridges. These features are indicative of stabilisation of the ice margin during overall retreat (Ottesen and Dowdeswell, 2006). The retreat ridges on Thor Iversenbanken are likely to have been formed by slow ice flowing from the east, over Thor Iversenbanken. Those in the upper parts of Sentralbankrenna are more likely to have been formed by ice flowing from Sentralbanken. The four larger retreat ridges in the channel and basin area on Thor Iversenbanken, have previously been interpreted as recessional moraines, indicative of a longer margin stillstand (Bjarnadóttir et al., 2014). Based on their geomorphic characteristics and setting we find it likely that the smaller ridges in this area also represent recessional moraines or smaller push moraines, although without subsurface data, their origin cannot been confirmed.

4.5. Short, flat imprints with sedimentary berms: Ice-fingerprints

4.5.1. Description

Along the north-western margin of Sentralbankrenna two areas have been mapped, to the west of GZW 5 (fig. 6 C) and upstream of GZD 7 (fig. 2 A and E), where the seafloor is characterised by elongate, semi-parallel, flat bottomed features that have lengths and widths ranging from

150-2500 m and 180-700 m, respectively. Many of these features terminate in long crescentic, asymmetric shaped berms, with heights between 1-6 m and widths of 100-450 m (fig. 6 C and D). These features appear downstream of the mapped retreat ridges (cf. section 4.4) as short and wide imprints, which overprint longer and narrower imprints that in some locations merge or turn into with curvilinear furrows without berms (cf. section 4.6; fig. 6 C).

4.5.2. Interpretation

These semi-parallel, flat-bottomed features with sedimentary berms on their downstream end are interpreted to be ice fingerprints, glacial features formed beneath an ice margin experiencing transverse extensional flow (Bjarnadóttir et al., 2014). The geomorphological sequence we observe in this area is as follows, 1) retreat ridges, 2) ice fingerprints, 3) furrows (in a distal to proximal order). This is similar to that observed in other locations within the Barents Sea (Bjarnadóttir et al., 2014) and in Iceland (Geirsdóttir et al., 2008). We suggest that these ice fingerprints may have been formed by an advancing ice cliff margin or icebergs characterised by fingers or sliver of ice, possibly during a period of extensive pervasive sea ice, which provided the buttressing needed for the ice margin to not break up directly into icebergs. Such a mechanism has been proposed for the formation of ice fingers in Iceland (Geirsdóttir et al., 2008).

4.6. Linear and curvilinear furrows: Iceberg ploughmarks

4.6.1. Description

The seafloor throughout much of Sentralbankrenna and the shallower bank areas is heavily scoured with many furrows of varying shapes and sizes (figs. 2 A, B, E and 7 A). On the shallower parts of Thor Iversenbanken and Sentralbanken, as well as on top of most of the large sedimentary deposits, there are several relatively narrow, randomly orientated curvilinear furrows, with a V-shaped cross-profile (fig. 7 B). Their widths range from ~65-210 m and their depths from ~0.5-10 m. Downstream of GZW 1 are several uniform, relatively narrow U-shaped furrows, with widths extending 70-125 m, depths between 0.75-6 m, and orientated ESE-WNW. Between GZW 1 and GZW 2 the furrows are less common, with fewer features mapped.

In mid- to upper-Sentralbankrenna, between GZW 2 and GZW 5 there are many semi-parallel curvilinear furrows orientated parallel to the troughs long-axis (fig. 2 A, B and E), many of the furrows between GZW 3 and GZW 5 display one of two distinct orientations (fig 7 A). The dominant orientation for the furrows in this area is NE-SW parallel to the trough long-axis, however, coming from Sentralbanken downstream of the retreat ridges and ice fingerprints to the west of GZW 5, there are several furrows orientated in a NW-SE direction. Both these sets converge in the mid-section of Sentralbankrenna at a water depth of 260-290 m (fig. 7 A), before following the dominant NE-SW orientation in a more uniform manner. Widths and heights of these furrows vary from 100-1500 m and 1-8 m, respectively (fig. 7 B). A clear downstream termination of furrows is, in most cases, not observed in the study area. Within some of the furrows in upper Sentralbankrenna, in particular those downstream of and overprinting GZW 5 (figs. 2 E), are several relatively regularly spaced (140-170 m), small sedimentary ridges that appear roughly perpendicular to the furrow length orientation, and have heights ranging from 0.5-2 m and widths from 150-300 m.

4.6.2. Interpretation

We interpret the furrows observed within the dataset to be iceberg ploughmarks, formed by the scouring of seafloor sediments by grounded iceberg keels. Such features have been documented extensively across formerly glaciated continental margins (e.g. Barnes and Lien, 1988; Kuijpers et al., 2007; Dowdeswell et al., 2010; Andreassen et al., 2014; Bjarnadóttir et al 2014; Dowdeswell and Hogan, 2014), and can be used to infer the proximity to the ice margin, with the assumption that more uniform scours suggest ice proximal icebergs and those randomly orientated indicative of ice distal icebergs whose path is dictated by the wind or ocean currents (Smith and Banke, 1983). Alternatively, it is possible that larger icebergs may be less sensitive to wind or ocean currents than smaller icebergs.

There are fewer iceberg scours between GZW 1 and GZW 2, than within the rest of upper Sentralbankrenna, possibly due to a deepening of the trough meaning that the calved icebergs keels did not reach the seafloor, or otherwise due to surface sediment cover in this area burying all but the deepest ploughmarks. The uniform ploughmarks visible on the seafloor between GZW 3 and GZW 5 (fig. 7 A) show two main source directions. Less dominant ploughmarks come from Sentralbanken in a NW-SE orientation and more dominant ploughmarks orientated N-S following the axis of Sentralbankrenna. It is possible that the ploughmarks between GZW

3 and GZW 5 may be obscuring older features, although this cannot be confirmed with the data currently available. We propose that the ice margin at GZW 5 may have been highly dynamic with a high calving rate based on the large quantity of ploughmarks downstream of the GZW; or alternatively that there was a rapid break-up of the ice margin when it was at GZW 3, and subsequent retreat from GZW 3 to GZW 5.

Within several of the furrows, in particular those present downstream and on top of GZW 5, are many short and linear ridges that run perpendicular to the scour marks (fig. 7 A). We interpret these to be corrugation ridges. Corrugation ridges have been identified in both palaeo- and contemporary environments (Solheim and Pfirman, 1985; Jakobsson, 2011; Graham et al., 2013; Andreassen et al., 2014). We infer that these features were formed by icebergs trapped in a dense ice matrix, where their keels squeezed the seafloor sediment into small ridges under a tidal regime (Jakobsson et al, 2011).

5. Discussion

5.1. The Sentralbankrenna glacial system

A complex assemblage of glacial landforms was mapped in the study area, composing of multiple grounding zone deposits, MSGLs, meltwater features and retreat ridges. Based on this geomorphological record we propose that the Sentralbankrenna glacial system experienced several retreats and/or readvances, each marked by a GZW or GZD, during the period of overall deglaciation since the LGM. The glacial system comprised of the fast flowing Sentralbankrenna Ice Stream and slower moving inter-ice stream ice masses located over northern Sentralbanken and northern Thor Iversenbanken (fig. 8A). In the southern part of Sentralbankrenna there are a number of meltwater features, suggesting that subglacial meltwater was abundant in this area and that basal hydrology may have played a key role in determining the location of ice streaming by facilitating lubrication of the ice stream bed.

In the following sections, we present a 6-stage reconstruction of the deglaciation of the Sentralbankrenna glacial system. Due to the poorly constrained chronology from the central Barents Sea, we are only able to provide a relative chronology for stages 2 – 6, however it seems plausible that the trough was deglaciated sometime after 16 cal ka BP (fig. 1; Winsborrow et al., 2010; Hughes et al., 2015).

621

622 *5.1.1. Stage 1 – LGM and early deglaciation*

623 Stage 1 relates to the LGM and early deglaciation, during which the BSIS was at its maximum
624 extent, reaching the shelf break. Several ice streams were active during this period (fig. 8 A);
625 the largest of these was the Bjørnøyrenna Ice Stream, which had tributaries of fast flowing ice
626 coming from Storbankrenna and Sentralbankrenna (fig. 8 A; Bjarnadóttir et al., 2014). During
627 maximum glacial conditions the Bjørnøyrenna Ice Stream was not topographically controlled,
628 as evidenced by the identification of east-west oriented MSGLs in central Bjørnøyrenna
629 (Piasecka et al., 2016) and supported by numerical modelling (Patton et al., 2016). The BSIS
630 was a multi-domed ice sheet, with a potential source for Sentralbankrenna being the ice dome
631 likely located over Storbanken, in the northern Barents Sea, and extending over Sentralbanken
632 towards the south-eastern Barents Sea (fig. 8 A; Patton et al., 2015; Piasecka et al., 2016).

633

634 *5.1.2. Stage 2 – Post LGM*

635 Stage 2 relates to an ice margin position associated with the deposition of GZW 1 (fig. 8 B).
636 During, or prior to, this stage Sentralbankrenna Ice Stream and Bjørnøyrenna Ice Stream
637 became separated by an inter-ice stream area overlying Sentralbanken, thus significantly
638 reducing the catchment area for Bjørnøyrenna Ice Stream. This separation was likely associated
639 with a northwesterly shift in source area for the Bjørnøyrenna Ice Stream (Andreassen et al.,
640 2014), potentially coinciding with an ice dome that has been suggested over Hinlopenstretet
641 (Dowdeswell et al., 2010; fig. 1), with the Sentralbankrenna Ice Stream likely still fed by an ice
642 divide located over Storbanken.

643 During this stage, the Sentralbankrenna Ice Stream flowed in an ENE-WSW direction, with its
644 ice margin marked by GZW 1 (figs. 1 and 8 B). Based on subsurface data, GZW 1 from this
645 study is a composite feature formed by four generations of GZW, indicating that this margin
646 may have been relatively stable during its initial retreat stage (Bjarnadóttir et al., 2014). Fast
647 flowing ice occupied the whole trough and continued even during the last phases of GZW
648 development, as evidenced by large MSGLs 1 and 2 (fig. 4 A) on the ice proximal side of the
649 wedge. On the adjacent shallower area of Thor Iversenbanken the geomorphology indicates the
650 presence of slower flowing, less active ice, coming from the southeast Barents Sea. A large

shear margin likely existed at the boundary between these two ice masses and this is marked by a clear slope break and abrupt end to the channels east of MSGLs 2 (fig. 8 A).

Meltwater coming from the channels and subglacial basins in southern Sentralbankrenna may have contributed to the location and dynamics of the Sentralbankrenna Ice Stream (fig. 8 B). The subglacial basins east of MSGL 2 are likely to have been active, connected and undergoing periods of rapid discharge and infilling, possibly on a seasonal timescale, similar to subglacial lakes in Greenland (Palmer et al., 2013) and in Antarctica (Fricker and Scambos, 2009; Smith et al., 2009). MSGL 1 are significantly larger than MSGL 2 (fig. 4 A) indicating that they may have been formed during the peak period of GZW 1 deposition, whereas MSGL 2 may have been formed as a product of ice stream flow switching. This could occur due to changes in water supply to the trough, or during the final stage of GZW 1 deposition prior to rapid margin breakdown and retreat back to GZW 2. Alternatively, MSGL 1 and 2 may represent a single ice stream event, where the ice stream has a more arcuate shape and MSGL 1 was positioned closer to the centre of the ice stream, where ice flow would have been faster.

5.1.3. Stage 3

The retreat from GZW 1 to GZW 2 was likely to have been relatively fast, prior to the ice margin stabilising and coming to another stillstand and marking the initiation of stage 3 (fig. 8 C). Tunnel valleys near the northern extent of GZW 2 have eroded through the deposit, indicating that these channels must have been active during the formation of the sedimentary deposit and that meltwater continued to play a significant role in the facilitation of ice streaming, contributing to the lubrication of the ice bed in the trough upstream of this margin.

During this stage, the channel areas on Thor Iversenbanken are unlikely to have contributed to the facilitation of fast flow of the Sentralbankrenna Ice Stream, however, they will have still played a role in the ice dynamics of the overlying Thor Iversenbanken inter-ice stream ice. It is unclear where the ice margin on Thor Iversenbanken was during this stage. However, based on the retreat ridges and recessional moraines identified in the channel and basin area we suggest periodic stillstands during the retreat across Thor Iversenbanken, and that the ice margin here may have been more of an ice cliff, in contrast to the ice margins forming GZW 2. Furthermore, we suggest that the subglacial basins would have continued to be active during this time,

undergoing periods of infilling and rapid discharge, however, probably at a much slower discharge rate than during stage 2.

5.1.4. Stage 4

Sentralbankrenna Ice Stream may not have been stable at GZW 2 for a significant amount of time before it retreated back to GZW 3, based on its less prominent morphology. The location of GZW 3 marks the start of stage 4 (fig. 8 D). GZW 3 extends across the trough and is not particularly prominent due to being heavily scoured and overprinted. Based on the eastern extent of GZW 3, which extends almost to GZW 4, it is likely that it was formed during the time when the Sentralbankrenna Ice Stream began to split away from the slower moving inter-ice stream ice over Thor Iversenbanken and deposited GZD 9 (fig. 2 E). Due to the large amount of scourmarks on the seafloor it is difficult to determine the ice flow direction for the deposition of GZW 3. This makes it unclear whether: 1) ice came from the Sentralbankrenna ice stream orientated ENE-WSW; or 2) the ice dynamics in the northeastern Sentralbanken, an area previously inferred to be occupied by slower moving ice (Bjarnadóttir et al., 2014), underwent a change in regime, from a slow-to-more active ice mass, thus causing it to rapidly readvance in a NW-SE direction and almost reach the ice on Thor Iversenbanken (fig. 8 D). However, based on the sequence of 1) retreat ridges, 2) ice fingerprints and 3) ploughmarks, as well as the general positioning of GZW 3, we infer that this GZW was likely formed by ice flowing from Sentralbanken, which may have buried and eroded older features (i.e. the possible continuation of ice margin towards GZW 4). The sudden change in ice dynamics within the inter-ice stream ice over Sentralbanken may be due to loss of buttressing from the Sentralbankrenna Ice Stream, which by this stage could have retreated back to GZW 4 or even GZW 5. Should this be the case, then we speculate that the ice from Sentralbanken had a relatively fast readvance into the trough prior to retreating back to shallower ground, where the ice margin stabilised and formed several retreat ridges at its front. Prior to its stabilisation, the ice front may have experienced high calving rates and during periods of pervasive sea-ice, sections of the ice front were able to extend forming ice-fingerprints before calving.

5.1.5. Stage 5

Stage 5 (fig. 8 E) relates to the deposition of GZW 5 by the Sentralbankrenna Ice Stream and to the retreat ridges seen in upper Sentralbankrenna downstream of GZD 7 deposited by inter-ice stream ice coming from northern Sentralbanken. There are clear uncertainties in regards to the overall ice margin position and extent in the trough during this stage. We suggest that ice coming from the northern part of Sentralbanken, in the inferred inter-ice stream bank area, may have had an ice cliff margin, been relatively stable and experiencing a slow retreat, based on the deposition of the small retreat ridges and then the larger recessional moraine (GZD 7; Figs. 2 E and 8 E).

GZW 5 is suggested to be an intermediate GZW as defined by Bjarnadóttir et al. (2013) and Shackleton et al. (submitted). With a highly dynamic ice margin, this GZW will have been deposited under different levels of margin stability across the ice front, with a distinct difference between the west and eastern section. Differing water depths and the presence/lack of subglacial meltwater may have led to the distinct character of deposits within these two areas.

GZW 5 clearly displays different morphologies from the east to the west, with the shallower eastern extent having a more characteristic symmetric wedge like shape most likely formed through a line source deposition and based on its size and morphology may have been stable for a long period or had considerable and/or rapid sediment deposition. Whereas the western extent of GZW 5, displays a radial fan-like shape located in the deeper part of the trough, formed by point source deposition, such as from a subglacial meltwater conduit. This western extent may have experienced periods of stability enabling the formation of such large ice proximal fans.

While it is clear that subglacial meltwater played a significant role in the formation of these fans, little indication for meltwater was observed in this area. However, since the western extent of GZW 5 was located in a deeper section of the trough, it is possible that this section of the ice margin had higher calving rates due to increased marginal buoyancy (e.g. processes suggested by Pelto and Warren, 1991; Benn et al., 2007), as supported by the dense area of iceberg ploughmarks downstream of this area (fig. 7 A). This area of the ice margin, in contrast to the shallower areas adjacent, will therefore have had ice funnelled into it, providing a low-pressure pathway for meltwater. Thus, the ice margin over the western part of GZW 5 is likely to have been extremely sensitive to oceanographic changes (i.e. sea temperature and sea-level), since it was located in the deeper section of the trough and thus, may have been the first area to have responded to environmental changes during this stage, forming a large embayment.

743 Overprinting the eastern side of GZW 5 are several large semi-linear iceberg ploughmarks
744 containing corrugation ridges. It is unclear whether the formation of these relates to an ice
745 margin break-up due to floatation caused by the infiltration and undercutting of warmer ocean
746 waters and/or to sea level rise into a subglacial margin cavity, or whether these ploughmarks
747 relate to a highly dynamic calving margin when the ice front was located at GZW 6 (c.f. section
748 5.1.6). In the case of the latter, large deep-keeled icebergs may have become stuck on the
749 shallower GZW 5 crest, possibly in conditions of pervasive sea ice, and been influenced by
750 tidal motion, forming the corrugation ridges through similar processes to that which are
751 suggested for similar observations in Greenland fjords (Amundson et al., 2010), on the northern
752 Svalbard shelf (Dowdeswell and Hogan, 2014) and in West Antarctica (Jakobsson et al, 2011;
753 Graham et al. 2013).

754 It is uncertain whether the ice margin over GZW 5 and the ice margin over the retreat ridges
755 downstream of GZD 7 were coeval. Although, we have inferred based on the direction and
756 density of iceberg ploughmarks downstream of GZW 5 that the ice margin may have extended
757 across the trough, with the ice front over the western part of GZW 5, having formed an active
758 calving bay (fig. 8 E).

759

760 *5.1.6. Stage 6 – final retreat phase*

761 Stage 6 is the final retreat phase in this reconstruction and relates to the northern-most mapped
762 GZW 6 and GZD 7 (fig. 8 F), which may have been active at the same time. During this stage,
763 the inter-ice stream ice was likely to have had a longer stillstand, enabling it to deposit a large
764 recessional moraine (GZD 7; Fig. 2 E). The narrow and high symmetric morphology of this
765 deposit indicates the possibility of an ice cliff as the ice margin, which underwent very little
766 calving, hence the clear preservation of the features downstream of this deposit. During a later
767 phase of deglaciation, this margin may have continued to retreat and migrate towards the
768 shallower bank areas, where it once again stabilised and began to exhibit slow retreat and
769 deposit retreat ridges.

770 GZW 6 is a very good example of a classic GZW (e.g. Dowdeswell and Fugelli, 2012; Batchelor
771 and Dowdeswell, 2015), with a dense area of MSGLs overprinting the ice proximal side of the
772 GZW, indicating that ice was very active and streaming until the final stages of the GZW
773 formation. Based on the asymmetric shape and large size of GZW 6, as well as the positioning

of MSGL 4, we infer that this was formed by rapid deposition of sediment when the Sentralbankrenna Ice Stream was undergoing a final advance/retreat cycle. It is likely that the Sentralbankrenna Ice Stream continued to be fed by the ice divide over Storbanken.

5.2. Influence of the Sentralbankrenna glacial system on the BSIS

The glacial fluctuations occurring within Sentralbankrenna would have significantly contributed to the overall dynamics of the BSIS, based on the large size (>30,000 km^2) and critical location within the central part of the former ice sheet. During the initial phase of deglaciation following the LGM, Sentralbankrenna Ice Stream acted as a tributary to the adjacent Bjørnøyrenna Ice Stream, and therefore likely had a strong influence on its behaviour (fig. 8A). However, this influence lessened as deglaciation continued into its later phases and we suggest that the two ice streams were separated by non-streaming ice located over Sentralbanken (fig. 8B), thus significantly reducing the catchment area for the Bjørnøyrenna Ice Stream.

Following the identification of several large grounding zone deposits, studies have suggested that the Bjørnøyrenna Ice Stream experienced episodic retreat (Andreassen et al., 2008; Winsborrow et al., 2010; Bjarnadóttir et al., 2014). Similarly, during the later phases of deglaciation in the central Barents Sea, when the ice was more topographically controlled, Sentralbankrenna Ice Stream underwent a step-wise, episodic retreat as inferred from the landform assemblages of large GZW in combination with MSGLs (fig. 8 B-F). This pattern of rapid ice break-up punctuated by short stillstands or readvances is consistent with a general model for marine ice stream retreat proposed by Ó Cofaigh et al. (2008) and Dowdeswell et al. (2008).

In the adjacent bank areas, Sentralbanken and Thor Iversenbanken, the landform assemblage observed is that of slower, non-streaming, inter-ice stream ice. The features observed in these areas are similar to those identified in other high latitude palaeo-inter-ice stream areas, such as in the northwestern Svalbard (Ottesen and Dowdeswell, 2009) and eastern Amundsen Sea Embayment (Klages et al., 2013). Bjarnadóttir et al. (2014) proposed the presence of a smaller, local ice dome located over north Sentralbanken and based on the geomorphology in our study area, we suggest that the ice flow direction is consistent with a persistent mass of ice over Sentralbanken.

The presence of meltwater features, such as tunnel valleys and subglacial basins, indicates that there must have been an extensive and active subglacial hydrological system, which strongly influenced the dynamics of the overlying ice by: 1) facilitating ice streaming through lubrication of the bed; and 2) promoting dynamic ice margin conditions (i.e. formation of western part of GZW 5). The presence of several large subglacial meltwater systems associated with high levels of meltwater discharge, such as the tunnel valleys, in combination with highly dynamic calving margins in the upper Sentralbankrenna, suggest that the ice was still dynamically active and warm based.

6. Conclusions

Unlike the western Barents Sea which has been extensively investigated, the central Barents Sea remains scarcely studied. Observations and insights gained in this study have contributed to the overall knowledge of the BSIS deglaciation, particularly during the later stages. Analysis of a new high resolution bathymetric dataset, presented in this study, revealed glacial landform assemblages related to both the former Sentralbankrenna Ice Stream and the inter-ice stream areas in the adjacent banks, Sentralbanken and Thor Iversenbanken, in the central Barents Sea. Several large GZWs and MSGLs, as well as many smaller grounding zone deposits and meltwater associated features were observed, forming the basis for a 6-stage reconstruction of the deglaciation since the LGM (fig. 8 A-F).

While Sentralbankrenna Ice Stream underwent episodic retreat, with periods of rapid ice break up punctuated by margin stillstands or short readvances, the bank areas underwent much slower retreat rates, allowing numerous retreat ridges and recessional moraines to be formed. Further, the observed glacial meltwater features (tunnel valleys and subglacial basins) suggest that subglacial meltwater was abundant in this central part of the former ice sheet. The activity of subglacial water is likely to have greatly influenced the dynamics of overlying ice, and we suggest that periodical fill/release of water from subglacial lakes might have facilitated fast flow both for the Sentralbankrenna and Bjørnøyrenna Ice Stream.

Acknowledgements

We would like to acknowledge Kartverket (the Norwegian Hydrographic Service), the Geological Survey of Norway and the MAREANO programme for the provision of this dataset, used here under a CC by 4.0 license (https://creativecommons.org/licenses/by/4.0/legalcode). This is a contribution to CAGE (Centre for Arctic Gas Hydrate, Environment and Climate) that is funded by the Research Council of Norway through the Centre of Excellence funding scheme grant no. 223259. Furthermore, we would like to acknowledge the editor and reviewer, Neil Glasser, and our second reviewer, Stephen Livingstone, for their insightful and constructive comments, which have greatly helped to improve this manuscript.

Figures

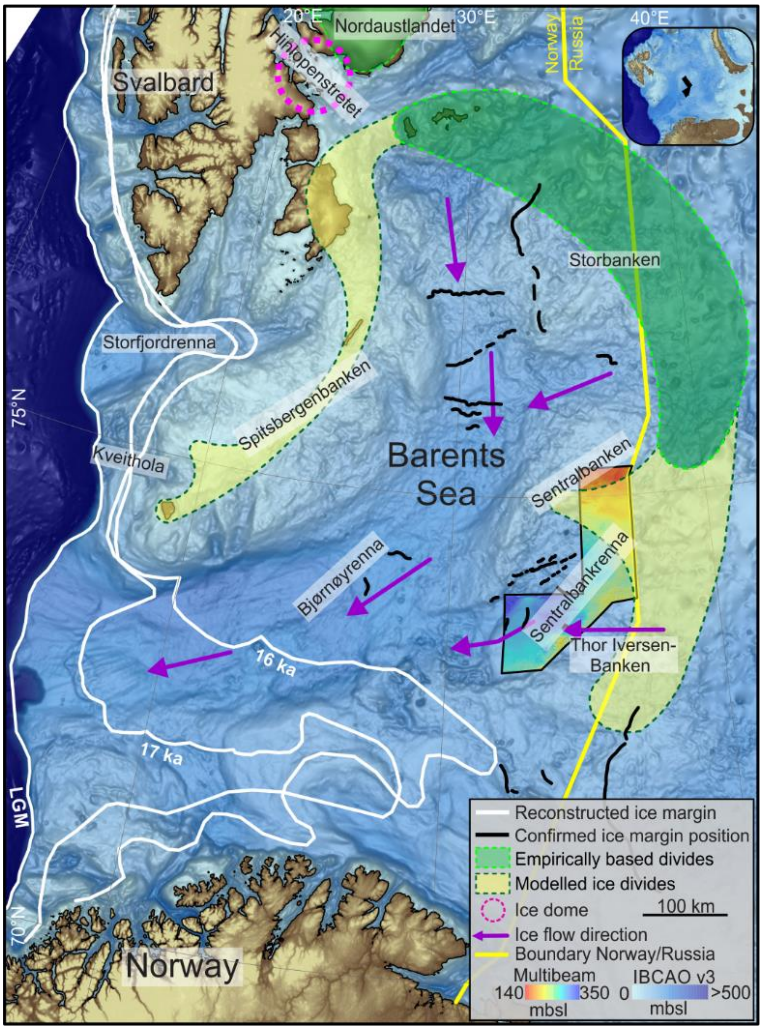

Figure 1. Map of the Barents Sea, showing the location of the study area (multibeam bathymetry: © Kartverket), the marine border between Norway and Russia, the Last Glacial Maximum (LGM;

Svendsen et al., 2004) and 17- and 16-cal ka BP ice margin extents (Winsborrow et al., 2010; extents north of Kveithola from Hughes et al., 2015), as well as the confirmed ice margin positions based on geophysical investigations (Rüther et al., 2012; Andreassen et al., 2014; Bjarnadóttir et al., 2014). The general ice flow directions are indicated by the purple arrows. The locations for the Storbanken ice divide (Bondevik et al., 1995 and Ottesen et al., 2005), its speculated extent over Sentralbanken/Thor Iversenbanken/Spitsbergenbanken (Patton et al., 2015) and the Hinlopenstretet ice dome (Dowdeswell et al., 2010) are also presented. Background bathymetry is from the International Bathymetric Chart of the Arctic Ocean (IBCAO) version 3.0 (Jakobsson et al., 2012). Inset map shows the location of the study area in relation to the whole Barents Sea.

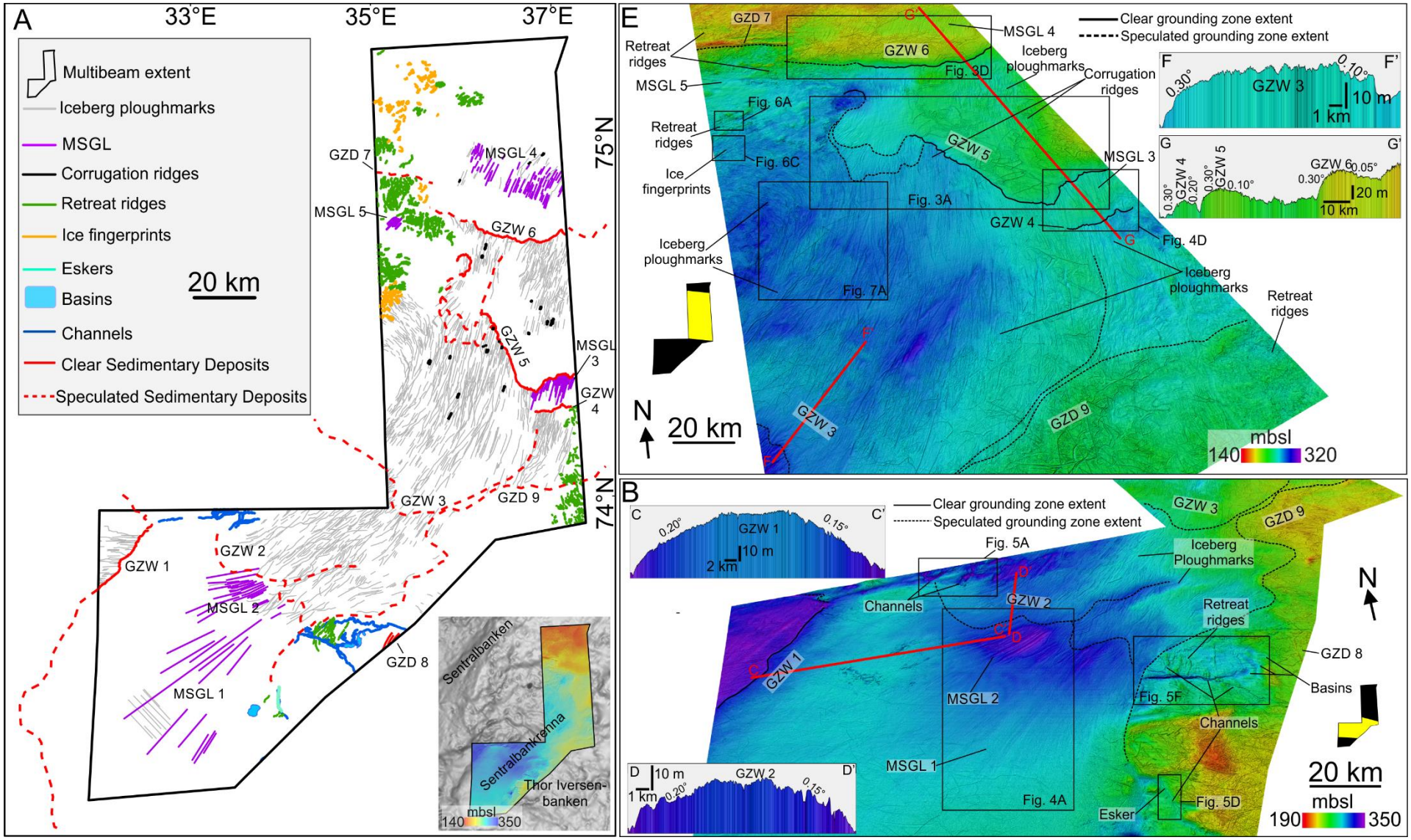
A
33°E
35°E
37°E
75°N
74°N
Multibeam extent
Iceberg ploughmarks
MSGL
Corrugation ridges
Retreat ridges
Ice fingerprints
Eskers
Basins
Channels
Clear Sedimentary Deposits
Speculated Sedimentary Deposits
20 km
GZD 7
MSGL 4
MSGL 5
GZW 6
GZW 5
MSGL 3
GZW 4
GZW 3
GZD 9
GZW 2
GZW 1
MSGL 2
GZD 8
MSGL 1
Sentralbanken
Sentralbankrenna
Thor Iversen-banken
mbsl
140
350
E
Clear grounding zone extent
Speculated grounding zone extent
Retreat ridges
Iceberg ploughmarks
Corrugation ridges
Ice fingerprints
Fig. 6A
Fig. 6C
Fig. 3A
Fig. 3D
Fig. 4D
Fig. 7A
F
F'
G
G'
0.30°
0.10°
10 m
1 km
0.05°
0.20°
20 m
10 km
N
20 km
mbsl
140
320
B
C
C'
0.20°
0.15°
2 km
Fig. 5A
Channels
Iceberg Ploughmarks
Retreat ridges
Fig. 5F
Basins
Fig. 5D
Esker
D
D'
1 km
Fig. 4A
190
350

857

Figure 2 (previous page). Geomorphology of the Sentralbankrenna glacial system. A – Mapped glacial landforms within the study area. B – Overview of the glacial landforms in the southern part of Sentralbankrenna within the multibeam data set (GZW – Grounding Zone Wedge; GZD – Grounding Zone Deposit; MSGL – Mega-Scale Glacial Lineation). C – Cross profile of GZW 1. D – Cross profile of GZW 2. E – Overview of the glacial landforms in the northern part of Sentralbankrenna. F – Cross profile of GZW 3. G – Cross profile over GZW 4, 5 and 6. Multibeam bathymetry: © Kartverket.

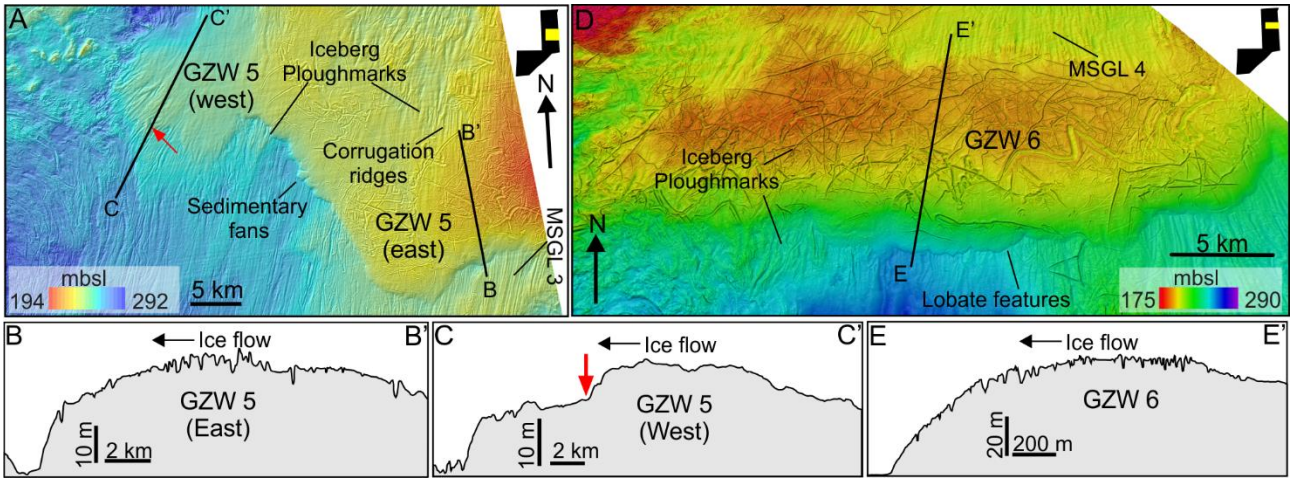

Figure 3. Grounding zone wedges in upper Sentralbankrenna. A – High resolution multibeam of GZW 5 showing several sedimentary fans, iceberg ploughmarks and corrugation ridges. B – Cross profile of the eastern side of GZW 5. C – Cross profile of the western side of GZW 5, with the red arrow pointing at the slope break and possible overlap with a second phase of wedge formation. D – High resolution multibeam of GZW 6, showing its lobate features on the ice distal side of the wedge, MSGL 4 and iceberg ploughmarks. E – Cross profile of GZW 6. Multibeam bathymetry: © Kartverket.

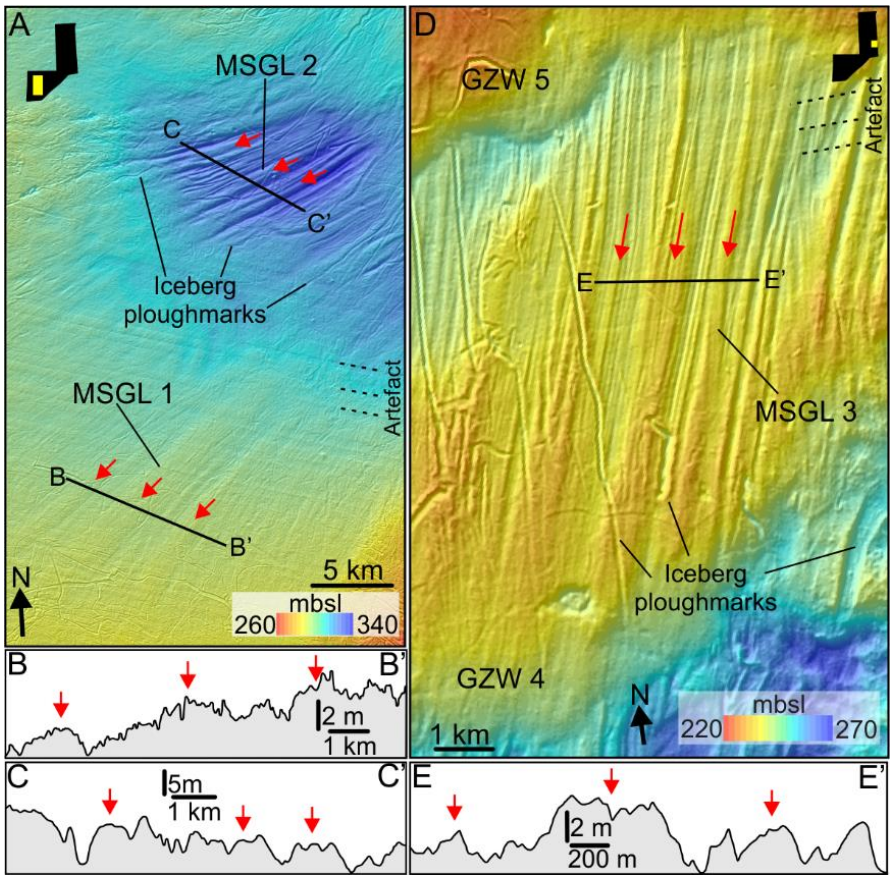

872

873 **Figure 4.** Mega-scale glacial lineations. A. Multibeam showing MSGL 1 and 2. B – Cross profile of
874 MSGL 1. C – Cross profile of MSGL 2. D - Multibeam of MSGL 3 overprinting the ice proximal side
875 of GZW 4. E – Cross profile of MSGL 3. The red arrows pointing to the positive feature of the MSGL.
876 Multibeam bathymetry: © Kartverket.

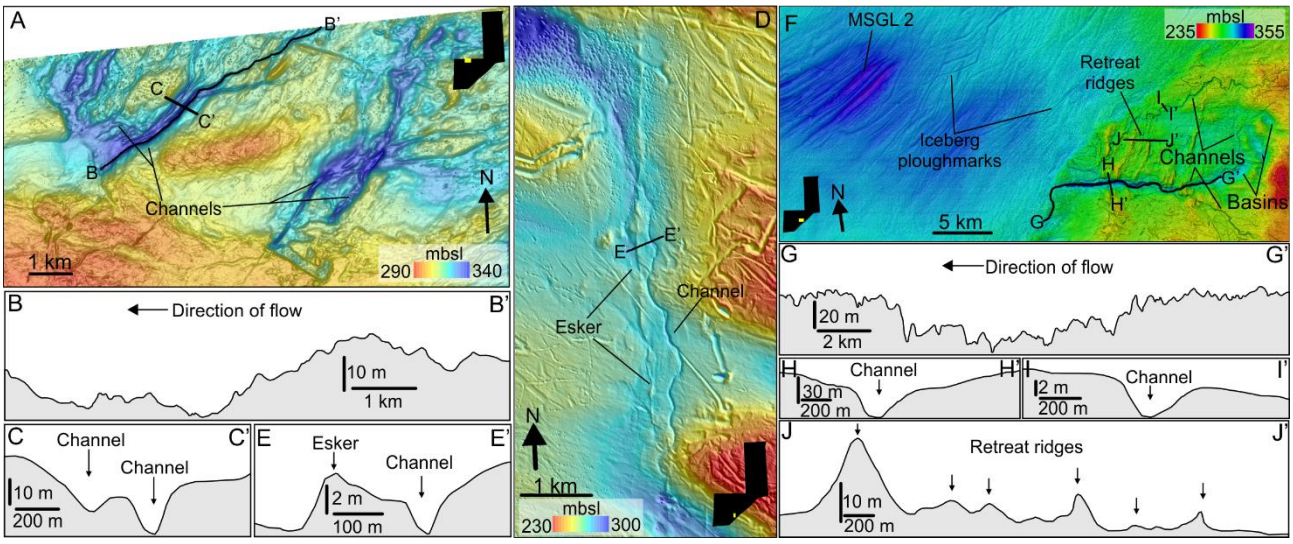

877

878 **Figure 5.** Meltwater channels and subglacial basins. A – Channel area to the north of GZW 2 showing
879 linked tunnel valley system (highlighted channels in the location map). B – Long profile of a tunnel
880 valley. C – Cross section of the tunnel valley. D - Channel area in the western part of Thor

Iversenbanken, showing a long sinuous channel with an esker running adjacent to it (highlighted channels in the location map). E Cross section of the channel and esker. F - Channel and basin area to the east of MSGL 2, showing a large tunnel valley (Bjarnadóttir et al., 2017) with several basins upstream from the main channel (highlighted channels in the location map). G – Long profile through the main central channel leading from the basins. H and I – Cross profiles of channels in the channel and basin area. J – Cross profile through the retreat ridges cross cutting the channels. Multibeam bathymetry: © Kartverket.

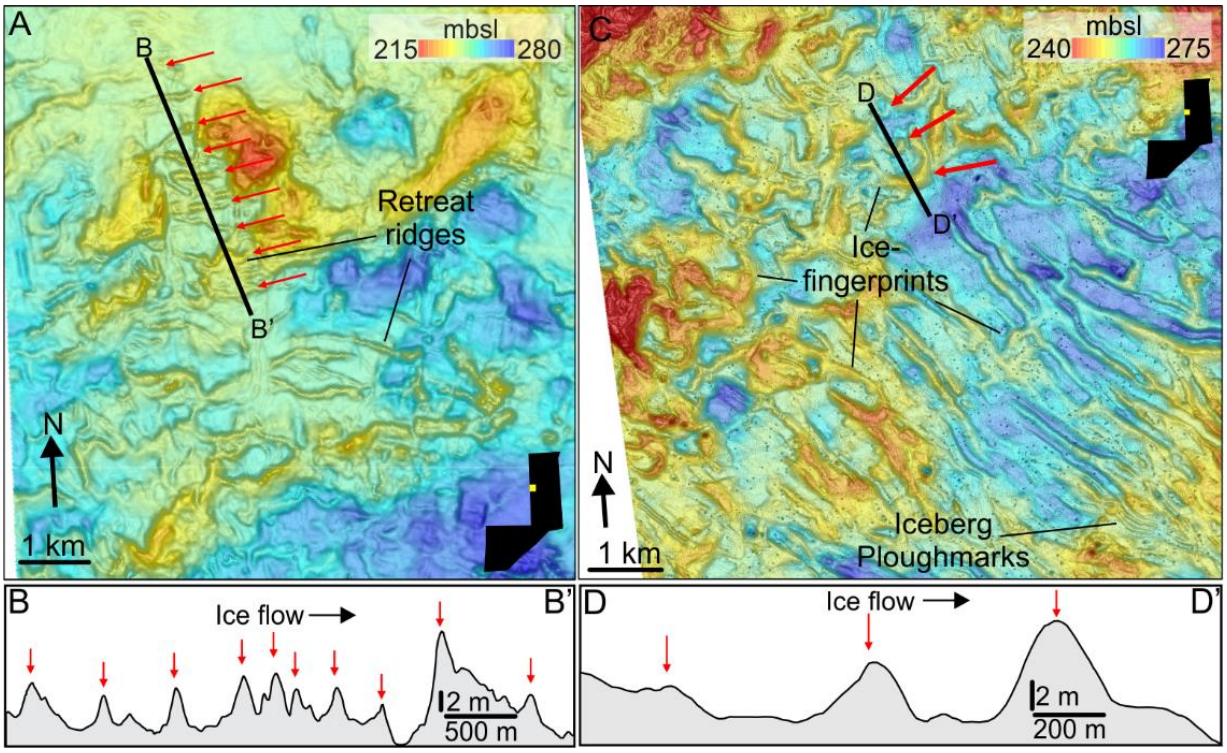

Figure 6. Ice-marginal features indicating slow retreat. A – Retreat ridges located to the west of GZW 5 (highlighted ridges in the location map). B – Cross profile of the ridges. C – Ice fingerprints downstream of the retreat ridges (highlighted features in the location map). D – Cross profile of the ice fingerprints. Multibeam bathymetry: © Kartverket.

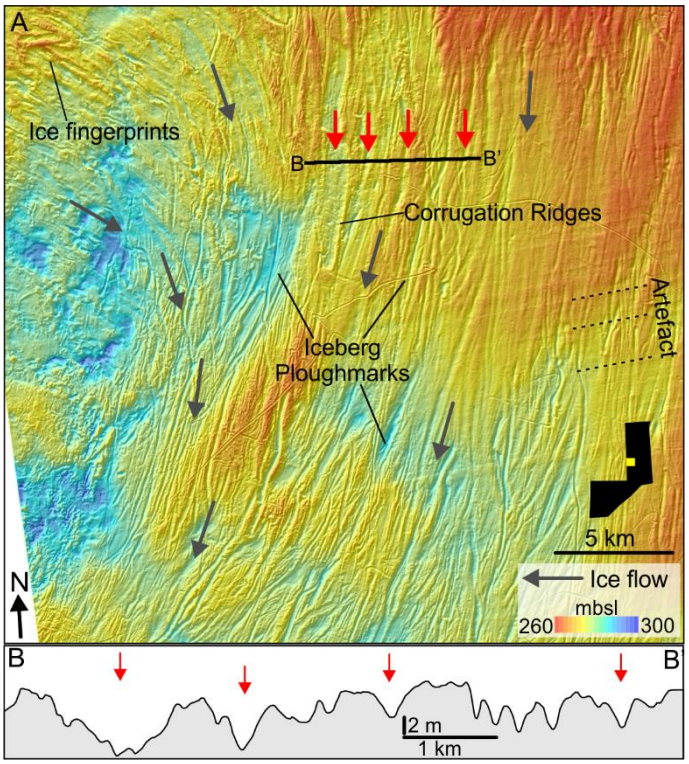

Figure 7. Iceberg ploughmarks and corrugation ridges. A – Iceberg ploughmarks between GZW 3 and GZW 5 (highlighted ploughmarks in the location map), showing the convergence between two different ploughmarks orientations (Grey arrow). Multibeam acquisition artefacts are highlighted by the dashed line. B - Cross profile of the ploughmarks. Multibeam bathymetry: © Kartverket.

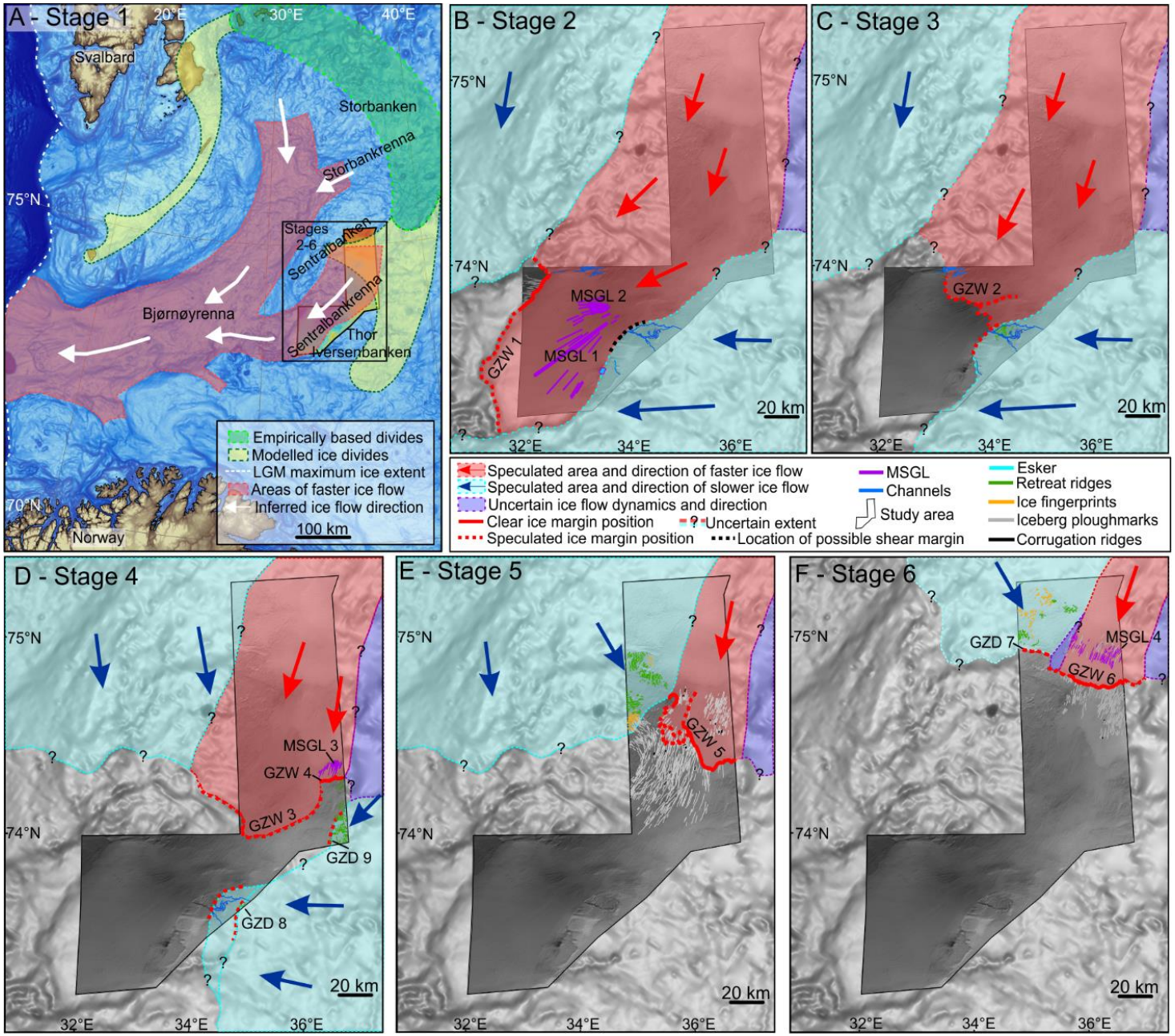
A - Stage 1
20°E
30°E
40°E
Svalbard
Storbanken
Storbankrenna
75°N
Stages 2-6
Sentralbanken
Sentralbankrenna
Bjørnøyrenna
Thor Iversenbanken
70°N
Norway
Empirically based divides
Modelled ice divides
LGM maximum ice extent
Areas of faster ice flow
Inferred ice flow direction
100 km
B - Stage 2
75°N
74°N
MSGL 2
MSGL 1
GZW 1
20 km
32°E
34°E
36°E
C - Stage 3
75°N
74°N
GZW 2
20 km
32°E
34°E
36°E
Speculated area and direction of faster ice flow
Speculated area and direction of slower ice flow
Uncertain ice flow dynamics and direction
Clear ice margin position
Uncertain extent
Speculated ice margin position
Location of possible shear margin
MSGL
Channels
Study area
Esker
Retreat ridges
Ice fingerprints
Iceberg ploughmarks
Corrugation ridges
D - Stage 4
75°N
74°N
MSGL 3
GZW 4
GZW 3
GZD 9
GZD 8
20 km
32°E
34°E
36°E
E - Stage 5
75°N
74°N
GZW 5
20 km
32°E
34°E
36°E
F - Stage 6
75°N
74°N
GZD 7
MSGL 4
GZW 6
20 km
32°E
34°E
36°E

902

Figure 8. 6-stage reconstruction of the ice dynamics in the Sentralbankrenna glacial system based on the glacial landforms mapped in the multibeam dataset. A – Stage 1, the BSIS LGM ice extent and ice dynamics showing: the areas of suggested fast flow and its flow direction (modified from Patton et al., 2015), LGM maximum ice extent (Svendsen et al., 2004), modelled ice divide (Patton et al., 2015), and the empirically based ice divides (Bondevik et al., 1995; Ottesen et al., 2005; Andreassen et al., 2014; Bjarnadóttir et al., 2014); B-F – Stage 2 – 6 of the Sentralbankrenna glacial system reconstruction and the mapped glacial features associated to each stage. Multibeam bathymetry: © Kartverket.

910 **Table 1**. Overview and comparison of grounding zone deposits. C.f. section 4.1 and 4.2 for further details and interpretations. Height is in relation to seafloor
911 downstream of feature. Length relates to that visible in the high-resolution bathymetry dataset as well as IBCAO bathymetry.

Descriptive name (c.f. section 4.1)	Location and orientation	Water depth (mbsl)	Height (m)	Width (km)	Length (km)	Distal/Proximal slope (°)	Key characteristics	Interpretation	Described in:	Present in figures:
Grounding Zone Deposit 1 (GZW 1)	Sentralbankrenna NE-SW	295	~35	~35-60	~100	0.20/0.15	• Dome-like shape (slightly asymmetric) • Four generations of GZW (Bjarnadóttir et al., 2014) • Overprinted by MSGL 1 and 2 in proximal slope • Breached by tunnel valley in its northern extent (Bjarnadóttir et al., submitted)	Grounding Zone Wedge	Bjarnadóttir et al. (2014) Newton and Huuse, 2017 This study	Figs. 2 A - C
Grounding Zone Deposit 2 (GZW 2)	Sentralbankrenna NW-SE	305	~10	~15	~45	0.20-0.79/0.15	• Dome-like shape (slightly asymmetric) • Subdued feature due to heavily scoured surface • Breached by tunnel valley in its northern extent Bjarnadóttir et al. (2017)	Grounding Zone Wedge	Bjarnadóttir et al. (2014) This study	Figs. 2 A, B and D
Grounding Zone Deposit 3 (GZW 3)	Sentralbankrenna NE-SW	265	~26	~15	~80	0.30/0.10	• Asymmetrical shape; steeper ice distal slope • Heavily scoured surface; overprinting and overprinted by iceberg ploughmarks • Uncertain extent (too dense scouring)	Grounding Zone Wedge	Bjarnadóttir et al. (2014) This study	Figs. 2 A, B, E and F
Grounding Zone Deposit 4 (GZW 4)	Sentralbankrenna W-E	235	~30	~10	~14	0.30/0.20	• Asymmetric shape • Overprinting many iceberg ploughmarks • Overprinted by MSGL 3	Grounding Zone Wedge	This study	Figs. 2 A, E, G and 4 D

Grounding Zone Deposit 5 (GZW 5)	Sentralbankrenna NW-SE	215 (East) 250 (West)	~31 (East) ~10 (West)	~30 (East) ~20 (West)	~35	0.30/0.10 (East) 0.20/0.10(West)	• Not a fully developed GZW, composed of several ice-proximal fans, particularly in the mid-sections and in the western side Eastern side: • Asymmetrical wedge-like shape • Overprinting MSGL 3 • Several high and prominent sedimentary fans where the feature extends west Western side: • Located in deeper part of trough • Radial fan-like deposit • Break in slope indicates a composite feature of two large fan-deposits • Steep ice distal side • Heavily overprinting and overprinted by iceberg ploughmarks	Intermediate Grounding Zone Wedge	Eastern part of GZW 5 described in Newton and Huuse, 2017 This study	Figs. 2 A, E, G and 3 A - C
Grounding Zone Deposit 6 (GZW 6)	Sentralbankrenna ESE-WNW	190	~60	~15	~37	0.30/0.05	• Well preserved • Prominent asymmetrical wedge-shaped feature • Overprinted by MSGL 4 • Overprinting several large iceberg ploughmarks downstream of the GZW • Several lobate features along its margin • Western extent subdued due to overprinting by other features	Grounding Zone Wedge	Newton and Huuse, 2017 This study	Figs. 2 A, E, G, and 3 D - E

Grounding Zone Deposit 7 (GZD 7)	Sentralbankrenna W-E	160	~50	~4	~20	1.50/0.75	• Less prominent asymmetrical shape • Narrow feature in comparison to GZW 1-6 • Several retreat ridges up and downstream of this moraine	Recessional Moraine	This study	Figs. 2 A and E
Grounding Zone Deposit 8 (GZD 8)	Located on Thor Iversenbanken NE-SW	240	~3-11	~200-340 m	~2-5	1.90/1.20	• Similar morphology to GZD 7 • Composed of three closely spaced symmetrical sedimentary deposits	Recessional Moraine	Bjarnadóttir et al. (2014) This study	Figs. 2 A and B
Grounding Zone Deposit 9 (GZD 9)	Located on Thor Iversenbanken NE-SW	220	~25	~8	~45	0.30/0.15	• Subdued feature due to being heavily scoured by iceberg ploughmarks • Morphology is clearer in the northern-most part of Thor Iversenbanken • Uncertain extent and unclear shape	Grounding Zone Deposit	Bjarnadóttir et al. (2014) This study	Figs. 2 A, B and E

912

913 References

914 Alley, R.B., Clark, P. U., Hybrechts, P., Joughin, I., 2005. Ice-sheet and sea-level changes.
915 Science. 310, 456–460.

916 Alley, R.B., Anandakrishnan, S., Dupont, T.K., Parizek, B.R., Pollard, D., 2007. Effect of
917 sedimentation on ice-sheet grounding-line stability. Science. 315, 1838–1841.

918 Amundson, J.M., Fahnestock, M., Truffer, M., Brown, J., Lüthi, M.P., Motyka, R.J., 2010. Ice
919 melange dynamics and implications for terminus stability, Jakobshavn Isbræ,
920 Greenland. J. Geophys. Res. Earth Surf. 115, 1–12.

921 Anandakrishnan, S., Catania, G.A., Alley, R.B., Horgan, H.J., 2007. Discovery of till deposition
922 at the grounding line of Whillans Ice Stream. Science. 315, 1835–1838.

923 Andreassen, K., Winsborrow, M., 2009. Signature of ice streaming in Bjørnøyrenna, Polar
924 North Atlantic through the Pleistocene and implications for ice-stream dynamics. Ann.
925 Glaciol. 50 (52), 17–26.

926 Andreassen, K., Nilssen, L. C., Rafaelsen, B., Kuilman, L., 2004. Three-dimensional seismic
927 data from the Barents Sea margin reveal evidence of past ice streams and their dynamics.
928 Geology. 32 (8), 729-732.

929 Andreassen, K., Laberg, J.S., Vorren, T.O., 2008. Seafloor geomorphology of the SW Barents
930 Sea and its glaci-dynamic implications. Geomorphology. 97 (1–2), 157–177.

931 Andreassen, K., Winsborrow, M., Bjarnadóttir, L.R., Rüther, D.C., 2014. Ice stream retreat
932 dynamics inferred from an assemblage of landforms in the northern Barents Sea. Quat.
933 Sci. Rev. 92, 246–257.

934 Auriac, A., Whitehouse, P. L., Bentley, M. J., Patton, H., Lloyd, J.M., Hubbard, A., 2016.
935 Glacial isostatic adjustment associated with the Barents Sea ice sheet: A modelling
936 inter-comparison. Quat. Sci. Rev. 147, 122-135.

937 Bamber JL, Vaughan DG, Joughin I., 2000. Widespread complex flow in the interior of the
938 Antarctic Ice Sheet. Science. 287, 1248–1250.

939 Barnes, P.W., Lien, R., 1988. Icebergs rework shelf sediments to 500 m off Antarctica.
940 Geology. 16, 1130–1133.

941 Batchelor, C.L., Dowdeswell, J.A., 2015. Ice-sheet grounding-zone wedges (GZWs) on high-
942 latitude continental margins. Mar. Geol. 363, 65–92.

943 Bell, R.E., 2008. The role of subglacial water in ice-sheet mass balance. Nat. Geosci. 1, 297–
944 304.

945 Bennett, M. R., 2003. Ice streams as the arteries of an ice sheet: their mechanics, stability and
946 significance. Earth-Science Rev. 61, 309–339.

947 Benn, D.I., Warren, C.R., Mottram, R.H., 2007. Calving processes and the dynamics of calving
948 glaciers. Earth-Science Rev. 82, 143–179.

949 Bindschadler, R., 2006. Hitting the ice sheets where it hurts. Science. 311, 1720–1721.

950 Bjarnadóttir, L.R., Winsborrow, M.C.M., Andreassen, K., 2012. Tunnel valleys in the Barents
951 Sea (Ph.D. thesis. In: Bjarnadóttir, L.R. (Ed.), Processes and Dynamics During
952 Deglaciation of a Polar Continental Shelf. Examples from the Marine-based Barents Sea
953 Ice Sheet. Geology Department, Faculty of Science and Technology, University of
954 Tromsø, Norway, ISBN 978-82-8236-080-7).

955 Bjarnadóttir, L.R., Rüther, D.C., Winsborrow, M.C.M., Andreassen, K., 2013. Grounding-line
956 dynamics during the last deglaciation of Kveithola, W Barents Sea, as revealed by
957 seabed geomorphology and shallow seismic stratigraphy. Boreas. 42, 84–107.

958 Bjarnadóttir, L.R., Winsborrow, M.C.M., Andreassen, K., 2014. Deglaciation of the central
959 Barents Sea. Quat. Sci. Rev. 92, 208–226.

960 Bjarnadóttir, L.R., Winsborrow, M.C.M., Andreassen, K., 2017. Large subglacial meltwater
961 features in the central Barents Sea. Geology. Doi: 10.1130/G38195.1.

962 Bondevik, S., J. Mangerud, L. Ronnert, O. Salvigsen., 1995. Postglacial sea-level history of
963 Edgeøya and Barentsøya, eastern Svalbard. Polar Res. 14(2), 153–180.

964 Christoffersen, P., Tulaczyk, S., Wattrus, N.J., Peterson, J., Quintana-Krupinski, N., Clark,
965 C.D., Sjunneskog, C., 2008. Large subglacial lake beneath the Laurentide Ice Sheet
966 inferred from sedimentary sequences. Geology. 36, 563–566.

967 Clark, C.D., 1993. Mega-scale glacial lineations and cross-cutting ice-flow landforms. Earth
968 Surf. Process. Landforms. 18, 1–29.

969 Dowdeswell, J.A., Fugelli, E.M.G., 2012. The seismic architecture and geometry of grounding-
970 zone wedges formed at the marine margins of past ice sheets. GSA Bulletin. 124, 1750–
971 1761.

Dowdeswell, J.A., Hogan, K.A., 2014. Huge iceberg ploughmarks and associated corrugation ridges on the northern Svalbard shelf. Geol. Soc. London, Memoirs.

Dowdeswell, J. A., N. H. Kenyon, A. Elverhøi, J. S. Laberg, F.-J. Hollender, J. Mienert, M. J. Siegert., 1996. Large-scale sedimentation on the glacier-influenced polar North Atlantic Margins: Long-range side-scan sonar evidence, Geophys. Res. Lett. 23(24), 3535–3538.

Dowdeswell, J.A., Ottesen, D., Evans, J., Ó Cofaigh, C., Anderson, J.B., 2008. Submarine glacial landforms and rates of ice-stream collapse. Geology. 36, 819–822.

Dowdeswell, J. A., Jakobsson, M., Hogan, K.A., O'Regan, M., Backman, J., Evans, J., Hell, B., Löwemark, L., Marcussen, C., Noormets, R., Ó Cofaigh, C., Sellén, E., Sölvsten, M., 2010. High-resolution geophysical observations of the Yermak Plateau and northern Svalbard margin: Implications for ice-sheet grounding and deep-keeled icebergs. Quat. Sci. Rev. 29(25–26), 3518–3531.

Elverhøi, A., Fjeldskaar, W., Solheim, A., Nyland Berg, M., Russwurm, L., 1993. The Barents Sea ice sheet – a model of its growth and decay during the last ice maximum. Quat. Sci. Rev. 12, 863–873.

Fricker, H. A., Scambos, T., 2009. Connected subglacial lake activity on lower Mercer and Whillans Ice Streams, West Antarctica, 2003-2008. Journal of Glaciology. 55 (190), 303–315.

Forman, S., 2004. A review of postglacial emergence on Svalbard, Franz Josef Land and Novaya Zemlya, northern Eurasia. Quat. Sci. Rev. 23, 1391–1434.

Fowler, A. C., 2010. The formation of subglacial streams and mega-scale glacial lineations. Proc. R. Soc. A. 466(2123), 3181–3201.

Graham, A.G.C., Larter, R.D., Gohl, K., Hillenbrand, C-D., Smith, J.A., Kuhn, G., 2009. Bedform signature of a West Antarctic palaeo-ice stream reveals a multi-temporal record of flow and substrate control. Quat. Sci. Rev. 28, 2774–2793.

Graham, A.G.C., Larter, R.D., Gohl, K., Dowdeswell, J.A., Hillenbrand, C.-D., Smith, J.A., Evans, J., Kuhn, G., Deen, T., 2010. Flow and retreat of the late Quaternary Pine Island-Thwaites palaeo-ice stream, West Antarctica. J. Geophys. Res. 115, F03025.

1000 Graham, A.G.C., Dutrieux, P., Vaughan, D.G., Nitsche, F.O., Gyllencreutz, R., Greenwood,
1001 S.L., Larter, R.D., Jenkins, A., 2013. Seabed corrugations beneath an Antarctic ice shelf
1002 revealed by autonomous underwater vehicle survey: Origin and implications for the
1003 history of Pine Island Glacier. J. Geophys. Res. Earth Surf. 118, 1356–1366.

1004 Geirsdóttir, Á., Miller, G. H., Wattrus, N. J., Björnsson, H., Thors, K., 2008. Stabilization of
1005 glaciers terminating in closed water bodies: Evidence and broader implications.
1006 Geophys. Res. Lett. 35, 1–5.

1007 Greenwood, S. L., Clason, C. C., Helanow, C., Margold, M., 2016. Theoretical, contemporary
1008 observational and palaeo-perspectives on ice sheet hydrology: processes and products.
1009 Earth-Science Rev. 155, 1-27.

1010 Hormes, A., Gjermundsen, E.F., Rasmussen, T.L., 2013. From mountain top to the deep sea –
1011 Deglaciation in 4D of the northwestern Barents Sea ice sheet. Quat. Sci. Rev. 75, 78–
1012 99.

1013 Hughes, A.L.C., Gyllencreutz, R., Lohne, Ø.S., Mangerud, J., Svendsen, J.I., 2015. The last
1014 Eurasian ice sheets - a chronological database and time-slice reconstruction, DATED-
1015 1. Boreas. 45, 1–45.

1016 Hulbe, C.L., Fahnestock, M.A., 2004. West Antarctic ice-stream discharge variability:
1017 mechanism, controls and pattern of grounding-line retreat. Journal of Glaciology. 50
1018 (171), 471–484.

1019 Ingólfsson, Ó., Landvik, J.Y., 2013. The Svalbard-Barents Sea ice-sheet-Historical, current
1020 and future perspectives. Quat. Sci. Rev. 64, 33–60.

1021 Jakobsson, M., Anderson, J.B., Nitsche, F.O., Dowdeswell, J.A., Gyllencreutz, R., Kirchner,
1022 N., Mohammad, R., O'Regan, M., Alley, R.B., Anandakrishnan, S., Eriksson, B.,
1023 Kirshner, A., Fernandez, R., Stolldorf, T., Minzoni, R., Majewski, W., 2011. Geological
1024 record of ice shelf break-up and grounding line retreat, Pine Island Bay, West
1025 Antarctica. Geology. 39, 691–694.

1026 Jakobsson, M., Anderson, J.B., Nitsche, F.O., Gyllencreutz, R., Kirshner, A.E., Kirchner, N.,
1027 O'Regan, M., Mohammad, R., Eriksson, B., 2012. Ice sheet retreat dynamics inferred
1028 from glacial morphology of the central Pine Island Bay Trough, West Antarctica. Quat.
1029 Sci. Rev. 38, 1–10.

1030 Jakobsson, M., Mayer, L., Coakley, B., Dowdeswell, J.A., Forbes, S., Fridman, B., Hodnesdal,
1031 H., Noormets, R., Pedersen, R., Rebesco, M., Schenke, H.W., Zarayskaya, Y.,
1032 Accettella, D., Armstrong, A., Anderson, R.M., Bienhoff, P., Camerlenghi, A., Church,
1033 I., Edwards, M., Gardner, J.V., Hall, J.K., Hell, B., Hestvik, O.B., Kristoffersen, Y.,
1034 Marcussen, C., Mohammad, R., Mosher, D., Nghiem, S.V., Pedrosa, M.T., Travaglini,
1035 P.G., Weatherall, P., 2012. The International Bathymetric Chart of the Arctic Ocean
1036 (IBCAO) Version 3.0. Geophys. Res. Lett. 39, LI2609.

1037 Jenkins, A., Doake, C.S.M., 1991. Ice-ocean interaction on Ronne Ice Shelf, Antarctica. J.
1038 Geophys. Res. 96, 791–813.

1039 Kehew, A.E., Piotrowski, J.A., Jørgensen, F., 2012. Tunnel valleys: concepts and controversies
1040 — A review. Earth-Science Rev. 113 (1–2), 33–58.

1041 King, E.C., Hindmarsh, R.C.A., Stokes, C.R., 2009. Formation of mega-scale glacial lineations
1042 observed beneath a West Antarctic ice stream. Nature Geoscience. 2, 585–588.

1043 Kirkbride, M. P., Warren, C. R., 1997. Calving processes at a grounded ice cliff. Ann. Glaciol.
1044 24, 116–121.

1045 Klages, J.P., Kuhn, G., Hillenbrand, C-D., Graham, A.G.C., Smith, J.A., Larter, R.D., Gohl, K.,
1046 2013. First geomorphological record and glacial history of an inter-ice stream ridge on
1047 the West Antarctic continental shelf. Quat. Sci. Rev. 61, 47–61.

1048 Kleiber, H.P., Knies, J., Niessen, F., 2000. The Late Weichselian glaciation of the Franz
1049 Victoria Trough, northern Barents Sea: ice sheet extent and timing. Mar. Geol. 168, 25–
1050 44.

1051 Kuijpers, A., Dalhoff, F., Brandt, M.P., Hümbs, P., Schott, T., Zotova, A., 2007. Giant iceberg
1052 plow marks at more than 1 km water depth offshore West Greenland. Mar. Geol. 246,
1053 60–64.

1054 Laberg, J.S., Vorren, T.O., 1995. Late Weichselian submarine debris flow deposits on the Bear
1055 Island Trough mouth fan. Mar. Geol. 127, 45–72.

1056 Lambeck, K., 1995. Constraints on the Late Weichselian ice sheet over the Barents Sea from
1057 observations of raised shorelines. Quat. Sci. Rev. 14, 1–16.

Lambeck, K., 1996. Limits on the areal extent of the Barents Sea ice sheet in Late Weichselian time. Glob. Planet. Change. 12, 41–51.

Landvik, J.Y., Bondevik, S., Elverhøi, A., Fjeldskaar, W., Mangerud, J., Salvigsen, O., Siegert, M.J., Svendsen, J.-I., Vorren, T.O., 1998. The last glacial maximum of Svalbard and the Barents Sea area: Ice sheet extent and configuration. Quat. Sci. Rev. 17, 43–75.

Livingstone, S. J., Ó Cofaigh, C., Stokes, C. R., Hillenbrand, C-D, Vieli, A., Jamieson, S. S. R., 2012a. Antarctic palaeo-ice streams. Earth-Science Rev. 111, 90–128.

Livingstone, S. J., Clark, C. D., Piotrowski, J. A., Tranter, M., Bentley, M. J., Hodson, A., Swift, D. A., Woodward, J., 2012b. Theoretical framework and diagnostic criteria for the identification of palaeo-subglacial lakes. Quat. Sci. Rev. 53, 88–110.

Livingstone, S. J., Stokes, C. R., Ó Cofaigh, C., Hillenbrand, C-D., Vieli, A., Jamieson, S. S. R., Spagnolo, M., Dowdeswell, J. A., 2016a. Subglacial processes on an Antarctic ice stream bed. 1: Sediment transport and bedform genesis inferred from marine geophysical data. Journal of Glaciology. 62 (232), 270–284.

Livingstone, S. J., Utting, D. J., Ruffell, A., Clark, C. D., Pawley, S., Atkinson, N., Fowler, A. C., 2016b. Discovery of relic subglacial lakes and their geometry and mechanism of drainage. Nat. Commun. 7:11767.

Mosola, A.B., Anderson, J.B., 2006. Expansion and rapid retreat of the West Antarctic Ice Sheet in eastern Ross Sea: possible consequence of over-extended ice streams? Quat. Sci. Rev. 25, 2177–2196.

Newton, A.M.W., Huuse, M., 2017. Glacial geomorphology of the central Barents Sea: Implications for the dynamic deglaciation of the Barents Sea Ice Sheet. Mar. Geol. 387, 114–131.

Ó Cofaigh C., 1996. Tunnel valley genesis. Progress in Physical Geography. 20(1), 1–19.

Ó Cofaigh, C., Dowdeswell, J.A., Allen, C.S., Hiemstra, J., Pudsey, C.J., Evans, J., Evans, D.J.A., 2005. Flow dynamics and till genesis associated with a marine-based Antarctic palaeo-ice stream. Quat. Sci. Rev. 24, 709–740.

Ó Cofaigh, C., Dowdeswell, J.A., Evans, J., Larter, R.D., 2008. Geological constraints on Antarctic palaeo-ice-stream retreat. Earth Surf. Process. Landforms. 33, 513–525.

1087 Oppenheimer, M., 1998. Global warming and the stability of the West Antarctic Ice Sheet.
1088 Nature. 393, 325–332.

1089 Ottesen, D., Dowdeswell, J.A., Rise, L., Rokoengen, K., Henrikson, S., 2002. Large-scale
1090 morphological evidence for past ice-stream flow on the mid-Norwegian continental
1091 margin. In: Dowdeswell, J.A., O´ Cofaigh, C. (Eds.), Glacier-Influenced Sedimentation
1092 on High-Latitude Continental Margins. Geological Society, London, pp. 245–258.
1093 Special Publication 203.

1094 Ottesen, D., Dowdeswell, J.A., Rise, L., 2005. Submarine landforms and the reconstruction of
1095 fast-flowing ice streams within a large Quaternary ice sheet: The 2500-km-long
1096 Norwegian-Svalbard margin (57-80N). GSA Bulletin. 117, 1033–1050.

1097 Ottesen, D., Dowdeswell, J.A., 2006. Assemblages of submarine landforms produced by
1098 tidewater glaciers in Svalbard. Journal of Geophys. Res. 111, F01016.

1099 Ottesen, D., Dowdeswell, J. A., 2009. An inter-ice-stream glaciated margin: Submarine
1100 landforms and a geomorphic model based on marine-geophysical data from Svalbard.
1101 GSA Bulletin. 121, 1647–1665.

1102 Palmer, S. J., Dowdeswell, J. A., Christoffersen, P., Young, D. A., Blankenship, D. D.,
1103 Greenbaum, J. S., Benham, T., Bamber, J., Siegert, M. J, 2013. Greenland subglacial
1104 lakes detected by radar. Geophys. Res. Lett. 40, 6154–6159.

1105 Patton, H., Andreassen, K., Bjarnadóttir, L.R., Dowdeswell, J.A., Winsborrow, M.C.M.,
1106 Noormets, R., Polyak, L., Auriac, A., Hubbard, A., 2015. Geophysical constraints on
1107 the dynamics and retreat of the Barents Sea Ice Sheet as a palaeo-benchmark for models
1108 of marine ice-sheet deglaciation. Rev. Geophys. 53, 1–48.

1109 Patton, H., Hubbard, A., Andreassen, K., Winsborrow, M., Stroeven, A.P., 2016. The build-up,
1110 configuration, and dynamical sensitivity of the Eurasian ice-sheet complex to Late
1111 Weichselian climate and ocean forcing. Quat. Sci. Rev. 153, 97–121.

1112 Pelto, M.S., Warren, C.R., 1991. Relationship between tidewater glacier calving velocity and
1113 water depth at the calving front. Ann. Glaciol. 15, 115–118.

1114 Piasecka, E.D., Winsborrow, M., Andreassen, K., Stokes, C.R., 2016. Reconstructing the retreat
1115 dynamics of the Bjørnøyrenna Ice Stream based on new 3D seismic data from the central
1116 Barents Sea. Quat. Sci. Rev. 151, 212–227.

1117 Polyak, L., Lehman, S.J., Gataullin, V., Timothy Jull, A.J., 1995. Two-step deglaciation of the
1118 southeastern Barents Sea. Geology, 23(6), 567–571.

1119 Powell, R.D., 1981. A model for sedimentation by tidewater glaciers. Ann. Glaciol. 2, 129–
1120 134.

1121 Powell, R.D., 1991. Grounding-line systems as second order controls on fluctuations of
1122 temperate tidewater termini. In: Ashley, G.M., Anderson, J.B. (Eds.), Glacial Marine
1123 Sedimentation — Paleoclimatic Significance. Geological Society of American Special
1124 Paper 261, pp. 75–94.

1125 Powell, R.D., Domack, E.W., 1995. Modern glaciomarine environments. In: Menzies, J. (Ed.),
1126 Glacial Environments: Volume 1. Modern Glacial Environments: Processes, Dynamics
1127 and Sediments. Butterworth-Heinmann, Oxford, pp. 445–486.

1128 Powell, R.D., Alley, R.B., 1997. Grounding-line systems: processes, glaciological inferences
1129 and the stratigraphic record. Geology and Seismic Stratigraphy of the Antarctic Margin,
1130 Part 2. Antarctic Research Series. 71, 169–187.

1131 Powell, R., Domack, E., 2002. Modern glaciomarine environments. In: Menzies, J.
1132 (Ed.),Modern and Past Glacial Environments. Butterworth-Heinemann, Boston, 361–
1133 389.

1134 Pritchard, H.D., Arthern, R.J., Vaughan, D.G., Edwards, L.A., 2009. Extensive dynamic
1135 thinning on the margins of the Greenland and Antarctic ice sheets. Nature. 461, 971–5.

1136 Rignot, E., Jacobs, S.S., 2002. Rapid bottom melting widespread near Antarctic ice sheet
1137 grounding lines. Science. 296, 2020–2023.

1138 Rignot E, Casassa, G., Gogineni, P., Krabill, W., Rivera, A., Thomas, R., 2004. Accelerated ice
1139 discharge from the Antarctic Peninsula following the collapse of the Larsen B ice shelf.
1140 Geophys. Res. Lett. 31, L18401.

1141 Rüther, D.C., Mattingsdal, R., Andreassen, K., Forwick, M., Husum, K., 2011. Seismic
1142 architecture and sedimentology of a major grounding zone system deposited by the

1143 Bjørnøyrenna Ice Stream during Late Weichselian deglaciation. Quat. Sci. Rev. 30,
1144 2776–2792.

1145 Rüther, D.C., Bjarnadóttir, L.R., Junttila, J., Husum, K., Rasmussen, T.L., Lucchi, R.G.,
1146 Andreassen, K., 2012. Pattern and timing of the northwestern Barents Sea Ice Sheet
1147 deglaciation and indications of episodic Holocene deposition. Boreas. 41, 494–512.

1148 Rydningen, T.A., Vorren, T.O., Laberg, J.S., Kolstad, V., 2013. The marine-based NW
1149 Fennoscandian ice sheet: glacial and deglacial dynamics as reconstructed from
1150 submarine landforms. Quat. Sci. Rev. 68, 126–141.

1151 Shackleton, C.S., Winsborrow, M.C.M., Andreassen, K., Bjarnadóttir, L.R., Submitted.
1152 Grounding zone dynamics of the Storfjordrenna Ice Stream, NW Barents Sea, inferred
1153 from ice margin landforms.

1154 Solheim, A., Pfirman, S.L., 1985. Sea-floor morphology outside a grounded, surging glacier:
1155 Bråsvellbreen, Svalbard. Mar. Geol. 65,127–143.

1156 Solheim, A., Andersen, E.S., Elverhøi, A., Fiedler, A., 1996. Late Cenozoic depositional history
1157 of the western Svalbard continental shelf, controlled by subsidence and climate. Global
1158 and Planetary Change. 12, 135–148.

1159 Siegert, M.J., Dowdeswell, J.A., Svendsen, J.I., Elverhøi, A., 2002. The Eurasian arctic during
1160 the last ice age. American Scientist. 90, 32–39.

1161 Smith, S.D., Banke, E.G., 1983. The influence of winds, currents and towing forces on the drift
1162 of icebergs. Cold Reg. Sci. Technol. 6, 241–255.

1163 Smith, B. E., Fricker, H. A., Joughin, I. R., Tulaczyk, S., 2009. An inventory of active subglacial
1164 lakes in Antarctica detected by ICESat (2003-2008). Journal of Glaciology. 50 (192),
1165 573–595.

1166 Stokes, C. R., Clark, C.D., 1999. Geomorphological criteria for identifying Pleistocene ice
1167 streams. Ann. Glaciol. 28, 67–74.

1168 Stokes, C. R., Clark, C.D., 2001. Palaeo-ice streams. Quat. Sci. Rev. 20, 1437–1457.

1169 Storrar, R. D., Stokes, C. R., Evans, D. J. A., 2014. Morphometry and pattern of a large sample
1170 (>20,000) of Canadian eskers and implications for subglacial drainage beneath ice
1171 sheets. Quat. Sci. Rev. 105, 1–25.

1172 Svendsen, J.I., Astakhov, V.I., Bolshiyanov, D.Y., Demidov, I., Dowdeswell, J.A., Gataullin,
1173 V., Hjort, C., Hubberten, H.W., Larsen, E., Mangerud, J., Melles, M., Möller, P.,
1174 Saarnisto, M., Siegert, M.J., 1999. Maximum extent of the Eurasian ice sheets in the
1175 Barents and Kara Sea region during the Weichselian. Boreas. 28, 234–242.

1176 Svendsen, J.I., Alexanderson, H., Astakhov, V.I., Demidov, I., Dowdeswell, J.A., Funder, S.,
1177 Gataullin, V., Henriksen, M., Hjort, C., Houmark-Nielsen, M., Hubberten, H.W.,
1178 Ingólfsson, Ó., Jakobsson, M., Kjær, K.H., Larsen, E., Lokrantz, H., Lunkka, J.P., Lysså,
1179 A., Mangerud, J., Matiouchkov, A., Murray, A., Möller, P., Niessen, F., Nikolskaya, O.,
1180 Polyak, L., Saarnisto,M., Siegert, C., Siegert, M.J., Spielhagen, R.F., Stein, R., 2004.
1181 Late Quaternary ice sheet history of northern Eurasia. Quat. Sci. Rev. 23, 1229–1271.

1182 Vorren, T.O., Kristoffersen, Y., 1986. Late Quaternary glaciation in the southwestern Barents
1183 Sea. Boreas. 15, 51–60.

1184 Vorren, T.O., Hald, M., Lebesbye, E., 1988. Late Cenozoic environments in the Barents Sea.
1185 Paleoceanography. 3, 601–612.

1186 Vorren, T.O., Laberg, J.S., 1997. Trough mouth fans – palaeoclimate and ice-sheet monitors.
1187 Quat. Sci. Rev. 16, 865–881.

1188 Wingham, D.J., Siegert, M.J., Shepherd, A.P., Muir, A.S., 2006. Rapid discharge connects
1189 Antarctic subglacial lakes. Nature. 440, 1033–1036.

1190 Winsborrow, M.C.M., Andreassen, K., Corner, G.D., Laberg, J.S., 2010. Deglaciation of a
1191 marine-based ice sheet: Late Weichselian palaeo-ice dynamics and retreat in the
1192 southern Barents Sea reconstructed from onshore and offshore glacial geomorphology.
1193 Quat. Sci. Rev. 29, 424–442.

1194 Winsborrow, M.C.M., Stokes, C.R., Andreassen, K., 2012. Ice-stream flow switching during
1195 deglaciation of the southwestern Barents Sea. GSA Bulletin. 124, 275–290.

1196